SEPTEMBER 2020

Ph.D. in Electrical and Electronics Engineering

ALIO AHMAT OUMAR

REPUBLIC OF TURKEY

GAZİANTEP UNIVERSITY

GRADUATE SCHOOL OF NATURAL & APPLIED SCIENCES

DEVELOPMENT OF A PHANTOM FOR QUALITY CONTROL OF A GAMMA CAMERA

Ph.D. THESIS

IN

ELECTRICAL AND ELECTRONICS ENGINEERING

BY

ALIO AHMAT OUMAR

SEPTEMBER 2020

DEVELOPMENT OF A PHANTOM FOR QUALITY CONTROL OF A GAMMA CAMERA

Ph.D. Thesis

in

Electrical and Electronics Engineering

Gaziantep University

Supervisor

Prof. Dr. Ergun ERÇELEBI

by

Alio AHMAT OUMAR

September 2020

©2020 [Alio AHMAT OUMAR]

I hereby declare that all information in this document has been obtained and presented in accordance with academic rules and ethical conduct. I also declare that, as required by these rules and conduct, I have fully cited and referenced all material and results that are not original to this work.

Alio AHMAT OUMAR

ABSTRACT

DEVELOPMENT OF A PHANTOM FOR QUALİTY CONTROL OF A GAMMA CAMERA

AHMAT OUMAR, Alio
Ph.D. in Electrical and Electronics Engineering
Supervisor: Prof. Dr. Ergun ERÇELEBI
September 2020
105 pages

This study deals with nuclear medicine as well as the technique of a gamma camera and the setting conditions in its good operation states, including associated with electronics, local materials, and test objects that can be employed for its calibration. Therefore, the thesis attempts to offer the nuclear medicine imaging field a novel phantom (imitation organ) and credibility of its possible uses. Additionally, the work describes the development method used to implement and test the phantom as a quality assurance tool. The phantom which is developed in this study can be considered as an original and valuable knowledge contribution made to the field. Since in-house phantoms may provide effective quality control for gamma cameras in clinical settings, in this thesis, it has been aimed at assess and develop an in-house phantom to perform quality control tests of a gamma camera using locally available, affordable materials. Such phantoms are especially important in developing countries where scientific support may not be readily available. The phantom which has been developed in the thesis was made from cylindrical plexiglass materials that are locally available and generally accessible to most nuclear medicine departments and require minimal engineering instruction. The phantom demonstrated high levels of reliability and accuracy. This work demonstrates that in-house phantoms are capable of monitoring gamma camera performance.

Keywords: Nuclear Medicine, Gamma Camera, Phantom, Quality Control, Protocol, Performance Test.

ÖZET

GAMA KAMERANIN KALİTE KONTROLÜ İÇİN BİR FANTOM GELİŞTİRİLMESİ

AHMAT OUMAR, Alio
Doktora Tezi, Elektrık-Elektronık Mühendisliği
Danışman: Prof. Dr. Ergun ERÇELEBI
Eylül 2020
105 Sayfa

Bu çalışma, nükleer tıbbın yanı sıra bir gama kamera tekniğini ve kalibrasyonu için kullanılabilecek elektronikler, yerel malzemeler ve test nesneleri dahil olmak üzere iyi çalışma durumlarındaki ayar koşullarını ele almaktadır. Bu nedenle, tez nükleer tıp görüntüleme alanına yeni bir fantom (taklit organ) ve olası kullanımlarının güvenilirliğini sunmaya çalışmaktadır. Ek olarak; bu çalışma, fantomu bir kalite güvence aracı olarak uygulamak ve test etmek için kullanılan geliştirme yöntemini açıklamaktadır. Bu çalışmada geliştirilen fantom, alana yapılan özgün ve değerli bir bilgi katkısı olarak kabul edilebilir. Ev içi fantomlar, klinik ortamlarda gama kameraları için etkili kalite kontrol sağlayabileceğinden, bu tezde, yerel olarak mevcut, uygun fiyatlı malzemeler kullanarak bir gama kameranın kalite kontrol testlerini gerçekleştirmek için bir ev içi fantomun değerlendirilmesi ve geliştirilmesi amaçlanmıştır. Bu tür fantomlar özellikle bilimsel desteğin hemen bulunamayacağı gelişmekte olan ülkelerde önemlidir. Tezde geliştirilen fantom, yerel olarak temin edilebilen ve çoğu nükleer tıp bölümü tarafından genel olarak erişilebilen ve minimum mühendislik eğitimi gerektiren silindirik pleksiglas malzemelerden yapılmıştır. Fantom, yüksek düzeyde güvenilirlik ve doğruluk gösterdi. Bu yaklaşım, bilimsel desteğe kolayca erişilemediğinde ve ticari fantomlar kolayca bulunamadığında özellikle yararlıdır.

Anahtar Kelimeler: Nükleer Tıp, Gama Kamera, Fantom, Kalite Kontrol, Protokol, Performans Testi.

"Dedicated to my parents"

ACKNOWLEDGEMENTS

Firstly, I would like to express my sincere gratitude to my supervisor Prof. Dr. Ergun Erçelebi for the continuous support of my Ph.D study and related research, for his patience, motivation, and immense knowledge. His guidance helped me in all the time of research and writing of this thesis. His suggestions and comments were central to the success of this project and I could not imagine without him this could be possible for my Ph.D study.

Besides my supervisor, I would like to thank the rest of my thesis committee: Prof. Dr. İlyas Eker, and Asst. Prof. Dr. Serkan Özbay, for their insightful comments and encouragement, but also for the relevant question which incented me to widen my research from various perspectives. I would also like to thank my committee members, Assoc. Prof. Dr. Tolgay Kara, and Asst. Prof. Dr. Abdulkarim Öztekin for serving as my committee members even at hardship. I also want to thank you for letting my defense be an enjoyable moment, and for your brilliant comments and suggestions, thanks to you.

My sincere thanks also go to Prof. Dr. Y. Zeki Çelen, the head of nuclear medicine department and staff for their cooperation, who gave me access to the nuclear medicine service. Without their precious support and permission it would not be possible to conduct this research.

I extend my sincere thanks to all members of the Department of Electrical and Electronics Engineering at the University of Gaziantep, and all those who contributed directly or indirectly to the dissertation. I want to say thank you to all my colleagues in the Department of Electrical and Electronics Engineering for their kindness and help. Also I want to thank all my friends for their encouragement.

Without the support of all members of my family, I would never finish this thesis and I would never find the courage to overcome all these difficulties during this work. My thanks go to my parents for their confidence and their love during all these years.

TABLE OF CONTENTS

LIST OF TABLES

Page

LIST OF FIGURES

Page

LIST OF SYMBOLS

Bq	Becquerel
Cm	Centimeter
cpm	Counts per minute
°C	Degree Celsius
ɣ	Gamma
GBq	Gigabecquere
hPa	Hectopascal
I	Iodine
Kg	Kilogram
Kcps	Kilo count per second
KeV	Kiloelectron-Volt
g/cm^3	Mass density
m	Metre
MBq	Megabecquerel
MeV	Megaelectron-Volt
µCi	Microcurie
mL	Milliliter
mm	Millimeter
%	Percentage
S	Second
^{99m}Tc	Technetium-99
θ	Theta

LIST OF ABBREVIATIONS

AAPM	American Association of Physicists in Medicine
AC	Air Conditioning/Alternating Current
ADC	Analog-to-Digital Converter
CB	Conduction Band
CFOV	Central Field of View
COR	Determination of Center of Rotation
CRT	Cathode Ray Tube
DU	Differential Uniformity
ECG	Electrocardiogram
FWHM	Full Width at Half-Maximum
GAUN	Gaziantep University
GM	Geiger-Muller
HV	High Voltage
IAEA	International Atomic Energy Agency
IEC	International Electrotechnical Commission
IU	Integral Uniformity
LFV	Large Field of View
NaI(TI)	Sodium Iodide doped with Thalium
NEMA	National Electrical Manufacturers Association
NM	Nuclear Medicine
PET	Positron Emission Tomography
PHA	Pulse Height Analyzer
PMT	Photomultiplier Tube
PMTs	Photomultiplier Tubes
PMMA	Polymethyl Methacrylate
QC	Quality Control

SD	Standard deviation
SPECT	Single-Photon Emission Computed Tomography
UFOV	Useful Field of View
2D	Two Dimensional
3D	Three Dimensional

CHAPTER I

INTRODUCTION

Nuclear medicine science is a branch of medicine that uses small amounts of radioactive material to diagnose or treat a variety of diseases such as, cancers and heart disease [1]. This is based on scintigraphic imaging for detection of ɣ radiation and the localization of photons emitted by radioactive decay within the patient. This technique is also called isotopic imaging (imaging by photons emission used for diagnostic purposes). It consists of evaluating the distribution of a radioactive substance into an organism administered to the patient by detecting the ɣ-ray, which it emits through an adaptive detective instrument or device [2, 3]. The latter is distinguished further from other medical imaging by its ability to non-invasively access information on the functioning of organs and to study their physiological and metabolic processes. Furthermore, the main difference between nuclear imaging and other radiologic diagnostic tests is that nuclear imaging investigates how an organ functions or a tissue behaves when injected by a molecule marked by a radioactive substance, whereas other imaging methods study the anatomy or how the organ looks. Thus, a functional image is produced by tracing the radioactive product. For instance, bone scan, injection of metastable technetium fixed on the bone [4-6]. This technique is accomplished using a large scintillation device, which was developed by H. Anger in 1958 and has been introduced to the field of nuclear medicine studies, which is called Anger camera, scintillation camera or ɣ-camera. Subsequently, the obtained images are recorded and documented in a computer system for further data processing. Hence, the purpose of radionuclide imaging is to obtain an image of the in vivo distribution of a radiotracer based on the external detection of high-energy photons emitted by radionuclide [7, 8].

Over the years, ɣ cameras have conferred many benefits to nuclear medicine applications in the fields of diagnostics, radiotherapy, and have privileged the doctors for the examination of the patient as well.

They also provided a variety of client services that are continuously evolving to meet the demand of the patients and physicians they serve. The availability of the radionuclide ^{99m}Tc and the evaluation of the ɣ imaging technology have led to the timely development of the SPECT (Single Photon Emission Computed Tomography) imaging technique [9-12]. As explained above, this technique is based on the detection of radiation and the location of photons emitted by radioactive decay within the patient. To obtain this information, a regular evaluation of the performance for the imaging system is required. Maintaining and improving the health and well-being of patients is achieved by providing the best care, qualified personnel, and reliable diagnostic instruments, which directly and indirectly contribute to patient satisfaction. Consequently, the presence of a quality control phantom within a nuclear medicine imaging department ensures the quality of the instrument and the safe care of the patient [13]. Furthermore, achieving a high standard of effectiveness and reliability in the practice of nuclear medicine necessitates a suitable quality control program to sustain a defined level of safety and to avoid error over time [14, 15]. Ideally, this could be carried out by all qualified personnel: a medical physicist, technician or maintenance engineer (trained on the device by the manufacturer), laboratory technician, and physician [16-18].

In order to carry out a comprehensive quality control procedure, different geometrically shaped phantoms are needed - including bars, spheres, line-sourced, and point-sourced - that can either be purchased commercially or built in-house. These phantoms can be filled with radioactive solutions and used to detect subtle changes in a gamma camera's performance prior to its clinical diagnostic use in order to avoid degradation in image quality [19-21]. Thus quality control procedures are important to maintain the quality of the provided diagnostic images. One of the most important parameters in need of daily testing is uniformity i.e., the ability of an imaging system to produce a uniform image when exposed to a homogeneous radioactive source. In general, this can be achieved either with a collimator (extrinsic) or without a collimator (intrinsic). As recommended by many

international organizations (e.g., National Electrical Manufacturers Association (NEMA), International Atomic Energy Agency (IAEA), similar to spatial resolution, the ability to display closely-spaced patterns of activity, image linearity and distortion, the ability to reproduce a straight line, should be confirmed six-monthly or at least annually, these can be performed either extrinsic or intrinsic [22-24].

NEMA (NEMA 2012) published a general approach to the routine quality control of gamma imaging systems before and after installation. It provides recommendations based on good clinical practices to support both the manufacturer and user communities [25, 26]. It describes how to carry out quality control procedures for a gamma camera with support and help from manufacturers. Often, all necessary phantoms can be conceptualized and realized in accordance with NEMA standards. Despite the availability of these standardized recommendations, practical implementation guidelines, and detailed instructions, it remains challenging for many nuclear medicine services to provide testing phantoms, which are required on a daily basis, due to the cost of materials or the lack of the required technology [27]. Moreover, phantoms utilized for quality assurance can be expensive and not always easily available and, as a consequence, quality control procedures cannot be performed [28]. The equipment can present inhomogeneity issues and may face problems related to maintenance and quality control for which additional scientific support is required. Ideally, the evaluation of gamma camera performance could be achieved using purpose-built phantoms that can be either purchased commercially or built in-house [29]. Therefore, there is a need for affordable phantoms that can be easily constructed and used during a routine basis if the quality control of SPECT systems is to be widely implemented [30, 31]. It is also of practical value to develop phantoms for routine testing using more accessible resources.

We hypothesize that an alternative in-house phantom can be used for routine quality control of a gamma camera. We also evaluated the phantom to establish its reliability by assessing the uniformity and certain performance parameters of the gamma camera. In addition, we compared the outcomes from the in-house phantom with those obtained from the point source of ^{99m}Tc, which are reflective of intrinsic uniformity. Nuclear medicine departments stand to benefit from this alternative and affordable way to make in-house phantoms suit their wishes and needs in accordance

with the NEMA guidelines, descriptions, and recommendations. Hence, this work describes the design and conceptualized use of such a phantom.

1.1 Motivation and Objectives

Gamma camera has become more common owing of its significance for imaging at the molecular level, especially in identifying the presence of diseases like cancer in their beginning levels. It can both detect cancer and determine its setback [32]. Quality Control is required to make sure that gamma cameras are functioning correctly and to detect problems before they affect clinical studies. Thus, it is relevant to carry out quality control tests in the gamma camera before running the experiment to prevent false results. Such tests regularly employ radioactive material inside phantoms for the assessment of gamma camera parameters in quality control procedures [33, 34]. Many studies have shown the importance of carrying out the quality control performance of a gamma camera. This should be carried out through phantom materials, as described by several international organizations such as NEMA, IEAE, IEC. This work motivates the importance of developing a quality control phantom to optimize the quality control process that checks the performance of the gamma camera. The procedure can be done by developing and improving in-house phantom techniques. It also utilizes readily available materials, which are comparatively affordable, accessible, and locally made and easy to use as a quality control device for gamma cameras performance testing [35,36]. Complete quality control of gamma cameras involves the performance of a variety of sophisticated system function tests, many of which demand expensive specialized equipment. A general phantom used for quality assurance can be expensive and not easily accessible. In addition, due to the fact that there are different gamma camera configurations and detector sizes, different phantoms will be required during tests. Thus, it will be of great benefit to nuclear medicine departments to have an alternative and cheaper way to manufacture phantoms according to their own needs. One of the motivations is to supply a daily basis needed devices that can be used to detect performance changes in a gamma camera system that may affect the interpretation of results in clinical studies. In some developing countries, at certain conditions, they face a lack of means to perform a constant quality control performance of their equipment, so there is a restricted amount of time that can be meaningfully used for system quality control. Obviously, we have a lot of factors

contributing to the final image quality, including uniformity, special resolution, collimation, energy resolution, contrast, and electronic devices. On top of that, for some types of studies other factors come into play, such as the sensitivity ability.

The purpose of this study is to analyze a newly developed in-house phantom based on the protocols proposed by manufacturers and user associations with local materials easily accessible. It is also to evaluate the efficiency of the locally manufactured phantom in the detection of ɣ camera malfunctions and compare it to the standard ones. Moreover, the aim is to show that this in-house phantom can be utilized to perform certain characteristics performance of a gamma camera.

1.2 Statement of the Problem and Contribution of the Thesis

Nowadays, NM represents one of the most important imaging methods and components of modern medical practice, using unsealed sources to give diagnostic information about diseases such as thyroid tumors. Besides imaging the internal state of a patient's body, it also provides both anatomical and biological functional information of organs within the body through gamma camera devices.

Significantly, a regular quality control testing and calibration of gamma cameras must be performed constantly to obtain good quality images without abnormalities and artifacts. Although most nuclear medicine departments perform routine quality controls in accordance with NEMA (NU 1-2007) standard protocol and IEC protocol, in most cases, the assessment in terms of validity and applicability of these tests is not performed. Specifically, in developing countries, imaging instruments can be installed with little or no funding for maintenance, QC and the provision of adequate scientific support. In such circumstances commercially made phantoms may be prohibitively expensive and as a result quality controls may not be implemented. Even when phantoms are available there are other restrictions to its use. For instance, many of the previously published and described QC procedures are complicated, time-consuming or require a specialized test environment, and specific software. There is also the lack of an independent quality control software manufacturer that can support the NEMA performance standard which is considered a major issue for running a NEMA quality control tests. Nonetheless, some parameters such as linearity, uniformity, special resolution, and energy resolution should be monitored regularly. Moreover, in gamma camera, an accurate model of its response is crucial to properly predict its performance and to acquire the best clinical

image results. Because of this an in-house phantom is designed and developed based on the international organization method. In addition, due to the fact that there are different gamma camera configurations and detector sizes, different phantoms will be required during tests. Thus, it will be of great benefit to nuclear medicine departments to have an alternative and cheaper way to manufacture phantoms according to their own needs. The final contribution of this dissertation is giving parametric knowledge of the methodology of developing a new phantom and its comparison to the conventional phantom's assessment of the performance of the gamma camera.

Finally, we found it necessary to develop an-house phantom that is user friendly for routine gamma camera testing and with an inexpensive cost in this research.

1.3 Outline of the Thesis

This dissertation consists of six chapters: Chapter one includes the introduction, motivation and objectives, statement of the problem and contributions of the thesis, and outline of the thesis. Chapter two includes theoretical background, nuclear medicine imaging and components of a gamma camera. Chapter three presents the QC and phantoms used in gamma cameras. Chapter four presents material and methods. Chapter five presents the results and discussion. Chapter six discusses the conclusion and references.

CHAPTER II

LITERATURE REVIEW

The acquisition of an image through a gamma camera is determined by the excellent use of a collimator, detector, and correct electronic settings, as each component in a gamma camera constitutes a liaison in a sequence. The conception of each component should not be handled alone. In this chapter, we present in sequence the literature review, which includes the historical and theoretical background of the gamma camera, and the basic physics of gamma photon and detection. We describe further, basic components and principles of a gamma camera and the main components implied in the formation of radionuclide imaging utilizing gamma radiation.

2.1 Historical Background

The first applications of nuclear medicine were developed in the mid-20th century, used Geiger-Muller (GM) counters which produced very low efficiency for the gamma photons (around 2%). In 1943, Seidling, Marinelli, and Oshry were treating patients who had thyroid cancer, with iodine 131, discovered that with the help of GM counter it is possible to locate the thyroid cancer metastases [37, 38].

In 1948, the research works of a German physician Heinz Kallmann have shown that the use of photomultiplier tubes (PMTs) associated with a scintillator crystal was much more efficient for the detection of the gamma rays [39]. Subsequently, Benedict Cassen, explored the substitution of Geiger-Muller tubes with scintillators and photomultiplier tubes [40, 41]. In 1957, Anger has invented the gamma camera, which has improved the development of diagnostic imaging in nuclear medicine. The fundamental conception, in which a thin sodium iodide detector is connected to an array of PMTs whose output is transmitted through a resistor matrix to generate image impulses, is basically not changed since the initial invention. The gamma camera has an advantage since it is a single device that can be employed for both dynamic and static studies.

The evolution of the gamma camera has been intimately associated with technetium-99m. Technetium-99m has the ability to emit a ɣ-ray and has a short half-life of six hours. It is facile to label (mark) with compounds for physiological, pharmacological and biochemical studies, as it bounds facilely with other materials.

Therefore, if the current gamma cameras have evolved, particularly in the level of their performances, yet the basic principle still based on Anger's camera. Today, a scintillation camera (also known as Anger camera, ɣ-camera or scintillation camera) constitutes a scintigraphic functional imaging technique, since its introduction by Hal Anger [42]. Thereafter, it has been undergone a great deal of progress in the development and improvement of methods to accurately quantify images in nuclear medicine. By the beginning of the 1970s was marked by continuous progress which leads to the invention of Single Photon Emission Computerized Tomography (SPECT), by which 3D images can be reconstructed. The gamma camera SPECT systems made of one or multiple head detectors bounded to a gantry structure contains several motorized movement axes that rotate around the human's body (patient) to acquire projection views and the system is coupled to a computer system that utilized to synchronize data collection with mechanical movements during acquisitions and both rebuilds and display the spatial resolution count density into 2D image on a monitor. The ɣ-camera with SPECT system has a main purpose, which is to scan heart, brain, liver, kidney and respiratory. It is applied for clinical investigations performing more excellently image and doing diagnosis easier [43].

2.2 Theoretical Background

A scintillation camera is an apparatus utilized to image ɣ radiation generating radioisotopes. This technique is recognized as scintigraphy, which was utilized in betimes medicine development and nuclear medicine imaging to visualize and analyze images of the human body or the distribution of medically injected, inhaled, or ingested radionuclide which emits ɣ rays.

Gamma cameras are able to detect radiation from the total field of view at the same time and for that reason are able of making static as well as dynamic images of the zone of interest in the body of the patient. Different designs of gamma cameras have been offered and made accessible; however, the Anger camera is by far most commonly utilized. Even though great sophisticated developments have been done on the gamma cameras over the years, the key principles of the functioning have

been fundamentally kept the same. They are made up of one or more heads optically coupled to an array of photomultiplier tubes. This is connected to a computer system, which controls the operation of the camera, acquisition, and storage of acquired images. The computer builds and displays a two-dimensional image of the proportional spatial count density on a monitor. This reconstructed image reflects the distribution and relative concentration of radioactive tracer elements present in the organs and tissues imaged [42].

2.3 Radioactivity

In nature, most of the nucleuses of atoms are stables. However, some nucleus atoms are unstable, which is because of either too many protons or too many neutrons, or too many of both. They are called radioactive and are called also radioisotopes or radionuclides. The nucleus of radioactive atoms transform spontaneously into other nuclei radioactive atoms or not (i.e., stable or unstable). When an unstable nuclei decays by losing energy through the emission of radiation in the form of alpha and beta particles, and gamma rays [43].

2.3.1 Gamma Decay

This decay is one kind of radioactive decay that a nucleus can undertake or go through. What makes this kind of decay action different from beta and alpha decay is that there is no particles are ejected from the nucleus during the gamma decay process. Rather, a high energy form of electromagnetic radiation: a gamma-ray photon is liberated. Gamma rays are just photons that have very high energies which are extremely high ionizing, with gamma being one the most strongly penetrating, as can be seen in Figure 2.1. Also, gamma radiation is specific in the sense that going through gamma decomposing does not modify the composition or structure of the atom. In lieu, it simply modifies the atom energy as the gamma-ray transfers no charge nor does it have an associated mass [44].

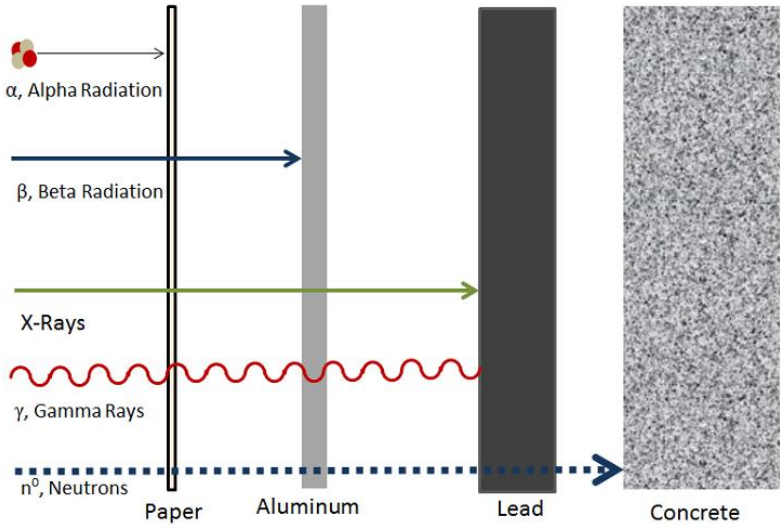

Figure 2.1 Various permeation levels of various products of decays [45].

So as for a nucleus to undertake gamma decay, it has to be in somehow of excited energetic state. Studies have demonstrated that protons and neutrons are localized in discrete energy states within the nucleus, not too different from the excited states that electrons can occupy in atoms. Therefore whether a proton or a neutron within the nucleus jumps up to an excited state, usually following an alpha or beta decay, thus the new daughter nucleus must in some sort liberate energy to permit the proton or neutron to remit back down to the ground state. During the transition made by the nucleon from high to low energy state, a gamma photon is released or emitted, as can be seen in Figure 2.2. This process is presented in the following expression:

$$A^* - A + \gamma \qquad (2.1)$$

where

A^* is the excited atom,

A is a relaxed state of the initially excited atom,

γ is the released gamma-ray photon.

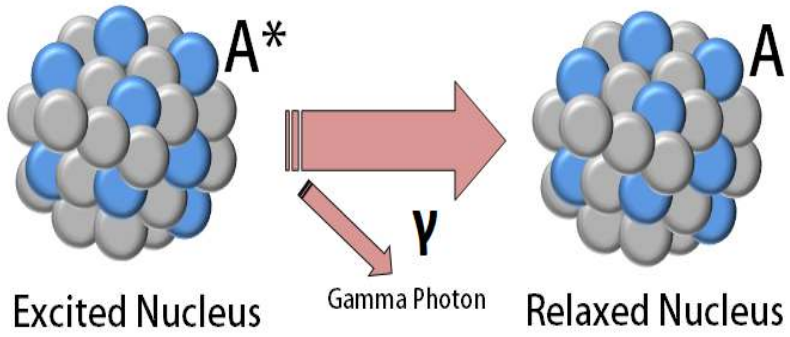

Figure 2.2 Schema showing gamma decay of a nucleus [45].

2.3.2 Radionuclides for Imaging

There exist several medical drugs can be labeled with radionuclides to make radiopharmaceuticals (radioactive tracers) [46, 47]. The administration of the radiopharmaceutical products leads the radionuclide to the desired tissue target or passageways. The administration is realized by injection, inhalation, or orally. The radiopharmaceutical (or the radioactive compound) is distributed into the body through the blood circulation. Over times the radiopharmaceutical will go and bind to the region of interest or organ. The small dose of radiopharmaceuticals employed, is in the order of nanograms and presents little impact upon the biochemical and physiological functions of the patient. For nuclear medicine imaging, the radionuclide used need to have suitable physical properties such as appropriate half-life, none particle emission, decay through emission with sufficiency enough energies to get through the body with less tissue attenuation, but quiet low to minimize the thickness of septa of the collimator [48, 49].

The ^{99m}Tc is the radionuclide that satisfies the most desirable criteria and is the most widely used radioisotope in diagnostic nuclear medicine, further utilized in more than 85% of all nuclear medicine studies. Because it is efficient at detecting cancer, cardiovascular, and other chronic diseases so that they can be treated. It is designed to seek out only tissues or organs, such as bones, heart, kidneys, among others. Moreover, it has a half-life of 6 hours and the absence of particle emission (such as alpha and beta) results in a less radiation dose to the patient. It also simple and quick to generate this radioactive source in a separator, known as a ^{99m}Tc generator [50].

2.4 Basics Physics of Gamma Photon and Detection

Gamma rays emitted by a radioelement or isotope will react with a matter, depend upon the photon energy and the atomic Z number of the material used, in which these interactions occur either with an electron medium or more rarely with a nucleus [51]. The difference in interactions results in subject contrast in imaging (radiology). The major types of interactions in the range of the energy employed in nuclear medicine are photoelectric effect, Compton effect, and pair production effect which is normally used in positron emission tomography (PET) technique. Therefore, each interaction of photon is going to deposit a part or the totality of its energy into the detector or patient tissue which contributes to patient dose, as shown in Figure 2.3 [52, 53].

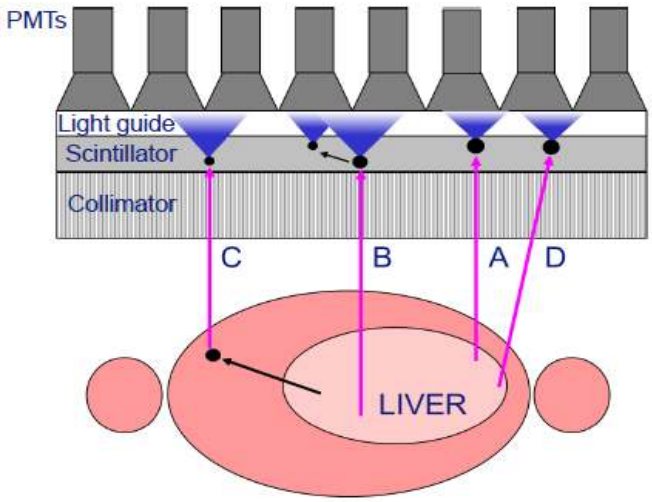

Figure 2.3 Patient with γ-emitting radionuclide concentrated in liver [53].

• A, valid event (a gamma-ray is emitted parallel to holes of the collimator, by passing through a hole of the collimator and interacting in the NaI(TI) crystal by photoelectric effect. It deposes all of its energy at a single location).

• B, detector scatter event (a gamma-ray is emitted parallel to holes of the collimator, by passing through a hole of the collimator and interacting in the NaI(TI) crystal by Compton scattering effect. The scattered gamma-ray can either interact a second time in the detector, deposing all of its energy, or may escape the detector, deposing only part of its energy).

• C, scattered in patient, because was not emitted toward to holes of the collimator, but subsequently is detected (γ-ray scatters in patient and may contain enough energy to fall in energy window: undesirable event).

• D, septal penetration (γ-ray travels through wall of collimator and reaches the detectors and interacts with it, but with a little chance that would occurring: undesirable event).

2.4.1 Photoelectric Effect

During the process of photoelectric effect, a gamma photon incident with energy E_0 is absorbed by the atom, as can be seen in Figure 2.4. This energy E_0 interacts with a bound electron, by transferring all the energy to the electron. Therefore, the gamma photon disappears and the atom thus emits an electron with an energy equivalent to the difference between the incident photon energy, E_0, and the bending energy E_1 of the electron. The kinetic energy of the photoelectron E_2, is given as follow:

$$E_2 = E_0 - E_1 \text{ or } E_0 = E_1 + E_2 \qquad (2.\ 2)$$

where E_0 is the gamma photon incident energy and E_1 is the bending energy. Usually, E_1 is smaller compared to the E_0, so as that the photoelectron carries out much of the photon energy. This effect can occur only that if $E_0 - E_1$ is greater than zero.

Therefore, for energies of diagnostic, photoelectric interactions are less susceptible to take place in soft tissues, which are mostly constituted from lighter compounds (lower Z). A greater energy photon will diminish the possibility of the photoelectric effect taking place as it will enter further into the matter. This is advantageous for image contrast and quality, because the interaction processes result in the absorption of the photon into the matter in the zone of low atomic number, result in attenuation [54, 55].

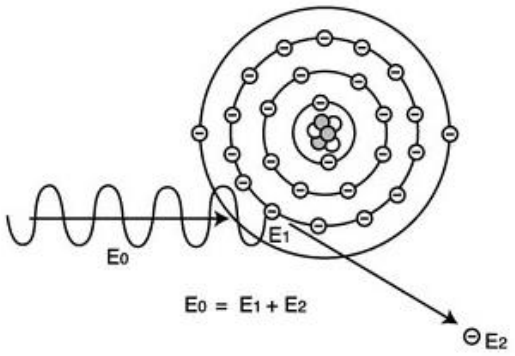

Figure 2.4 Photoelectric effect [54, 55].

2.4.2 Compton Effect

An incident photon of energy E_0 interacts directly with an atomic electron, this incident energy, instead of being absorbed completely, it rather ejects an electron, as can be seen in Figure 2.5. Since the energy of the incident photon is largely greater than the binding energy of the electron. In particular, this Compton effect happens between a photon and a valence electron (i.e. outer shell) and produces a scattered photon with a decreased energy. Hence, the scattered photon and the electron are ejected from the atom. Due to the conservation of energy and momentum, the energy of the incident photon, E_0, is equivalent to the energetic sum of the scattered photon (Esc) and the ejected electron (Ee-), expressed as follow:

$$Ee- + E_0 = Esc - Ee- \tag{2. 3}$$

Due to the binding energy or original of the ejected electron is small, it can be neglected. This ejected electron also can lose its energy along with the exciting and ionization mechanism with other atoms in the material. Particularly, the scattered photon can pass through the material free of further interactions or may go through subsequent interactions, such as scattering or absorption. Therefore, the energy of the scattered photon can be a function of the incident photon energy and the scattered photon angle θ:

$$Esc = \frac{E_\gamma}{1+\left(\frac{E_\gamma}{m_0 c}\right)(1-\cos\theta)} \tag{2. 4}$$

with

Esc is the energy after collision,

Eɣ is the energy before collision,

m_o is the electron rest mass,

θ is the scatter angle.

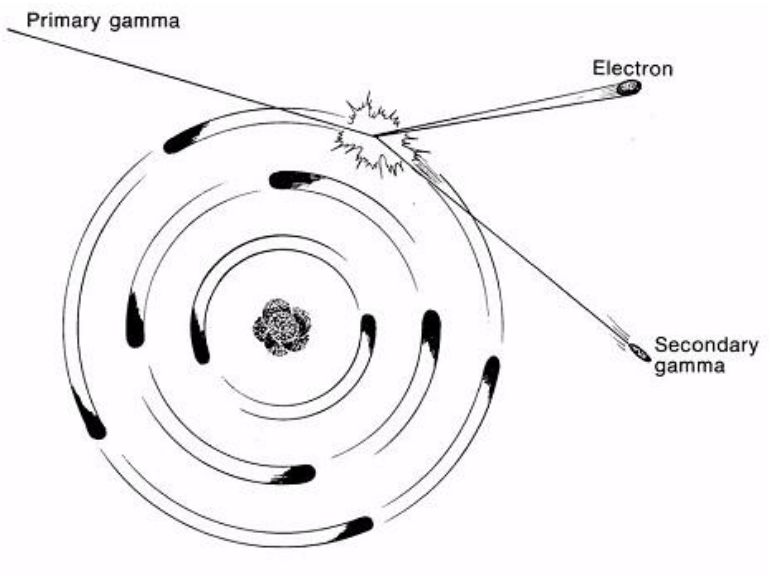

Figure 2.5 Compton effect [54,55].

2.4.3 Pair Effect

Pair effect is a result of an interaction between incident photons with matter. This effect can occur only when the energy of the incident gamma photon is sufficiently strong and superior to the equivalent energy of two-electron rest masses. It requires a minimum energy twice of 0.511 MeV which is 1.02 MeV. The gamma-ray can produce an electron and positron pair in the immediate proximity of an atomic nucleus. Subsequently, during the interaction, the photon energy is transferred into kinetic energy of 2 charged particles, a positron and an electron, as can be seen in Figure 2.6. These particles liberate their kinetic energy back into the medium by excitation and ionization. When the positron gets to rest, it will interact with an electron, creating in an annihilation reaction that makes two oppositely directed photons. These photons can be detected and are relevant for nuclear medicine imaging applications, particularly for PET techniques [54, 55].

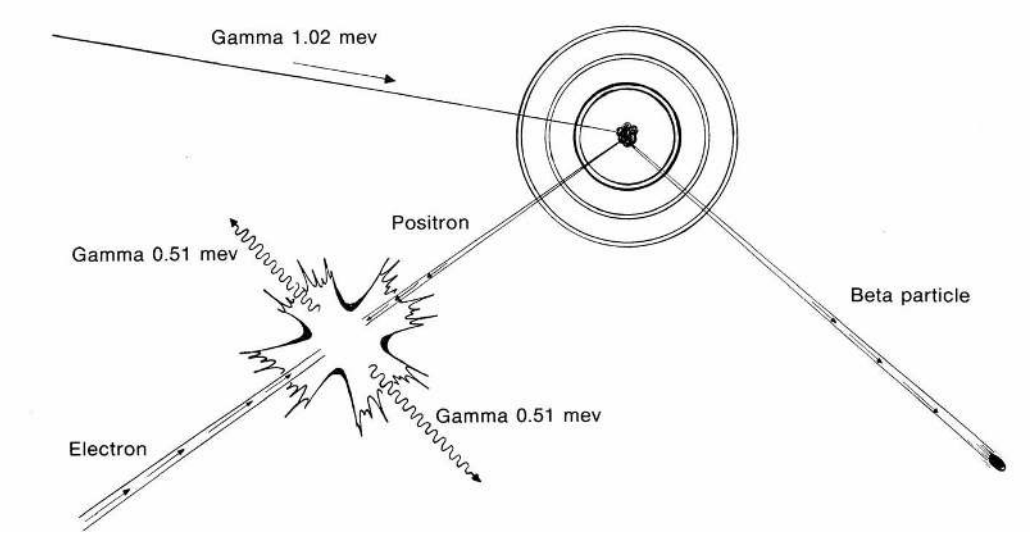

Figure 2.6 Pair effect [54, 55].

2.5 Basic Principles of a Gamma Camera

The gamma camera is an imaging apparatus using a thin and large diameter thallium activated sodium iodide Nal(TI) crystal viewed by an array of PMTs as a radiation detector.

The principle is based on the employ of radionuclide, which emits photons in a patient or a test object (or a phantom), the photons attain the crystal after traveling through a lead collimator which selects the photons coming from perpendicular direction to the detector of the gamma camera as well as defines the angle of acceptance. The scintillator crystal is coupled from its rear surface, either through a light guide or directly, to a set of PMTs. The PMTs are fed from a common High Voltage (HV) supply. At each tube, the gain of the voltage is slightly adjustable. The gamma rays, which are invisible to the naked eye, after passing through the collimator, a photon hits the surface of the crystal and interacts with it at a given spatial location, determines an X-Y coordinate system, this photon generates at the point of interaction a light scintillation which spreads through the crystal (IAEA 1991). The amount of these lights emitted from the scintillator interacts with the photocathode of a PM tube changes inversely with the distance of the PMT from the point of interaction and releasing electronic signals. The distribution of the amplitude of the impulses of all the PMTs, in the array owing to a single photon interaction, provides the location information.

The pulse signals from all the PMTs need to pass through an individual preamplifier for impulse shaping. These signals are then amplified with the help of an amplifier. Thereafter, the signals are sent at the same time to X and Y, and Z circuits. The signals X and Y are networks that provide the pulse amplitudes in ratio to the X and Y location of the initiating PMT in the coordinate system. The two analog signals, which are X and Y, with amplitudes ratio to the spatial coordinate of the event of the initial scintillation.

In the Z circuit, the signals are added up to produce in a Z signal corresponding to the all energy released in the crystal by the photon interaction (i.e., by the radiation). Given the intensity of the scintillation and thus the PMT output augments with photon energy, the X and Y signal need to be normalized so that the positional information is not dependent upon the photon energy. This is carried out in the energy correction circuit by dividing the X and Y signals by the Z signal (IAEA 1991).

The Z signal goes to a Pulse Height Analyzer (PHA), which tests if the energy of the gamma-ray is in the range of expected values for the specific radionuclide being imaged, i.e., if the Z signal meets in the PHA window set for the nuclide in use, The PHA allows the X/Z and Y/Z signals to record the event. If the Z signal has allowable value, then a signal is transmitted and later processed by a computer directly connected to the gamma camera, giving the display to record [56].

2.6 System Description

The system of a gamma camera is made with many components, each component carries out as a particular role in transforming gamma rays into light images and we ultimately obtain accurate viewing image. The main components of a ɣ-camera are the collimator, scintillation crystal, PM, PHA, signal processing, correction circuits, and image display. The gamma rays should travel via the collimator which makes certain that they pass through at a specified angle in accordance to the detector crystal. As can be seen in Figure 2.7, the ɣ rays passing through a collimator and getting to the scintillation crystal, for the first conversion into visible lights (photons). An array of PMTs then converts photon in electric signals that can be developed to produce the final image [57, 58].

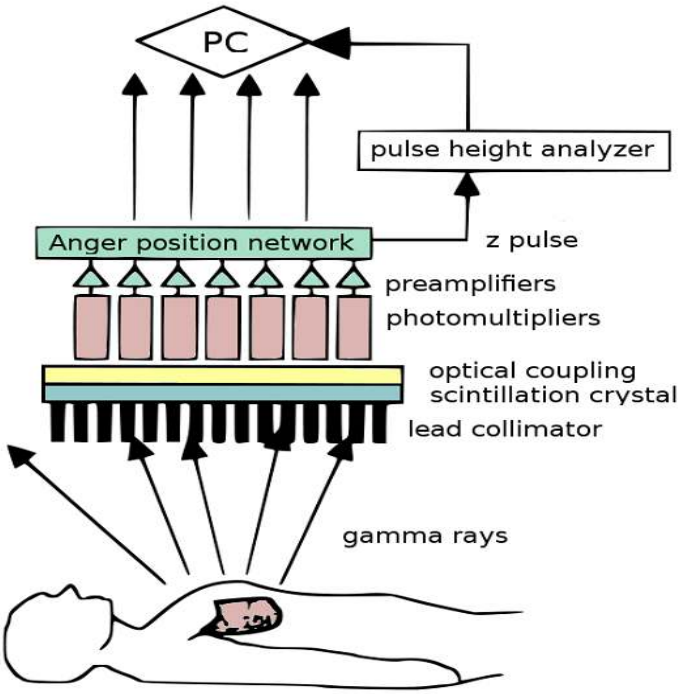

Figure 2.7 Basic components of an Anger gamma camera.

2.6.1 The Collimator

The collimator is made up of folded lead and is placed between the scintillation crystal and the patient. It permits the ɣ-camera to direct correctly the radionuclide in the body of the patient. Collimators carry out or play this role by absorbing and stopping maximum radiation apart from that coming particularly perpendicular to the face of the detector. Therefore, a collimator has a relevant part to play, which is to deny radiations coming from outside of the field of view and preventing them to reach the detector. Great gamma radiation hitting the collimator at oblique angles is not contributed to the final image. Almost all the photons emitted by an administrated radioactive material (radiopharmaceutical), almost all of them around 99% are lost and not taken in the count by the ɣ-camera; approximately one percent (1%) are utilized to produce the intended image. Therefore the collimator is the rate-limiting point in the imaging sequence of ɣ-camera technology. The Figure 2.8 shows the collimator action with the incident radiations that pass through it to get the detector. (a) scattered photon, (b) absorbed photon, (c) accepted photon, (d) septal penetration. Thus, for accurate image quality, it is relevant that the component (c) should be as large as possible comparing to (a) and (d) components which they cause a parasitic background noise lowering the image contrast.

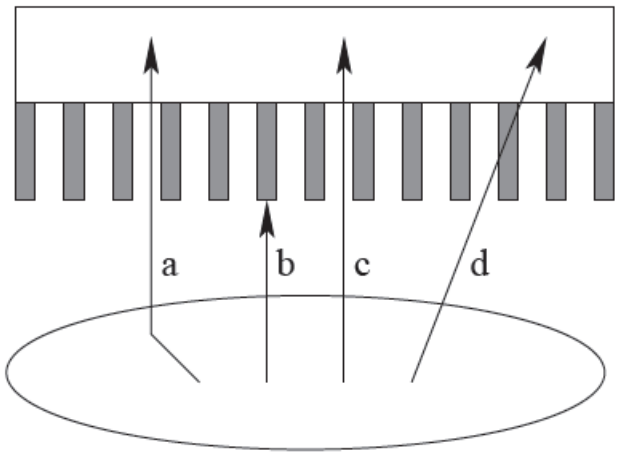

Figure 2.8 Incident radiations that pass through collimator to get the detector.

There are two basic types of collimators: are pinhole and multihole, as can be seen in Figure 2.9. A pinhole collimator functions similarly to that of a box camera, as shown in Figure 2.9 (a). Gamma-ray has to travel through the pinhole opening to be pictured, and the image is regularly inverted on the sodium iodide detector (the scintillation crystal). Small amount of the ɣ-ray from the object of interest is permitted to travel via the pinhole during a given time, the pinhole collimator affects the sensitivity of the ɣ-camera, i.e. has poorer sensitivity. The sensitivity of the collimator describes the percentage (%) of incident photons that travel across the collimator. The pinhole collimator poor sensitivity makes positioning close the organ of interest critical, and making the object of interest near to the pinhole magnifies the image. Since enlargement is a function of distance, if the object of interest is not relatively thin or flat, the image may be deformed. Pinhole collimators are regularly utilized for highly resolution images of little organs, such as the thyroid, and for some skeletal areas, such as wrists or hips, particularly in pediatric patients.

In a multihole collimator, the holes can be lined up in a parallel, diverging, or converging form, as shown in Figure 2.9 ((b) parallel, (c) diverging, and (d) converging). In nuclear medicine laboratories, the collimator with parallel hole is the most broadly utilized which is a multihole collimator. It is made up of parallel holes with a long axis at right angles to the plane (perpendicular) of the scintillation crystal. The lead walls between the holes are represented as septa. The septa take in most ɣ rays that do not derive from the direction of interest; so for high energy ɣ rays, a collimator has considerably thick septa and for low energy rays has less thick

septa. The septa are mostly made so that septal penetration by undesired ɣ rays does not surpass 10% to 25%.

A parallel hole collimator has to be selected to match the energy of the radionuclide being imaged and the type of the clinical examination. Low energy collimators usually refer to a maximum energy of 150 KeV, while medium energy collimators have a maximum recommended energy of about 400 KeV. Collimators are available with various widths of septa and sizes and shapes drilled through it. Generally, when the length of the septa is longer, the resolution is much better, but the lower the sensitivity for a given amount of radioisotope. The sensitivity (count rate) is reciprocally relative to the square of the collimator hole length. Whether the length of the septa is diminished, the detected sensitivity (count rate) augments, and resolution diminishes.

The difference between typical low energy, general-purpose collimators, and low-energy, high-sensitivity collimators is that high-sensitivity collimators may permit about double as many counts to be imaged, albeit the spatial resolution is generally deteriorated by about fifty percent. A high resolution, low energy collimator has about three times the resolving capability of a high sensitivity, low energy collimator.

With a parallel hole collimator, neither the sensitivity (count rate) nor the magnitude or dimension of the image modifies importantly with the distance of the object of interest from the collimator. This is owing to the fact that the object is being shifted a little distance away from the crystal, the inverse square law decreases the number of counts. On the other hand, this is recompensed for by the augmented viewing zone of the collimator. On the one hand, the resolution is better when the object of interest is as near as to the face of the collimator as possible, and scans with multihole collimators are generally acquired with the collimator in contact with or as near as possible to the patient. With a parallel hole collimator, scattered photons emitted from the patient perpendicular to the crystal meet may be imaged. These photons and those that penetrate the septa deteriorate septal resolution [59-61].

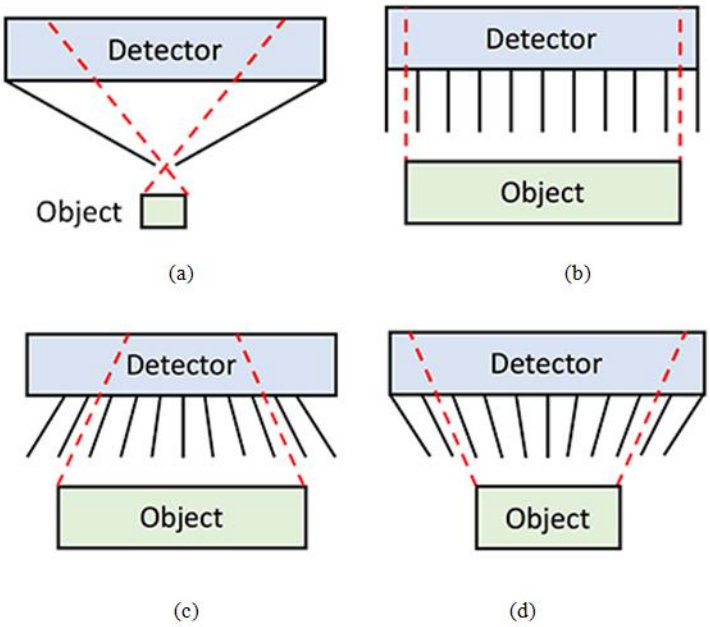

Figure 2.9 Collimators: (a) pinhole, (b) parallel, (c) diverging, and (d) converging hole [59-61].

2.6.2 Scintillation Detection

As the collimators modify the ɣ-rays flow such as to reproduce an image, it is the role of the detector assembly to transform the ɣ-rays into a form that will, ultimately, permit an observable image to be created. This process occurs in two steps. The first step is the transformation of the ɣ-rays into visible light through a scintillation crystal, whilst in the second step, these scintillations (visible lights) are converted into electrical signals through the PMTs.

The purpose of a scintillation detection system is to transform ɣ photons into an electrical signal which can be then utilized to analyze the energy of radiation and recording of events.

The scintillation detection consists of two components: it is firstly made with a sodium iodide NaI(TI) crystal which generates photons in a various part of the electromagnetic spectrum (410 wavelength which corresponds to the blue light at which the crystal is transparent and photocathodes of PMs sensible) after taking in all or most of the energy of the ɣ photons. The second component is the PMTs which can use this change in wavelength and transform the electromagnetic radiation into photoelectrons by the photoelectric effect.

A sodium iodide crystal doped with a very small amount of thallium NaI (TI) is most commonly used for ɣ-ray detection. The selection of crystals NaI (TI) for ɣ-ray detection is first-line due to their rational density (3.67g/cm^3). There are existing different types of NaI (TI) crystals utilized in gamma cameras as scintillators, they can be either in circular or rectangular shapes. For the portable cameras and mostly cardiac systems, crystals with a small field of view (30 cm) are employed. Crystals with a large field of view are used for multipurpose systems. Their dimensions vary from 30 to 60 cm in diameter for gamma camera with a circular field of view and from 50 to 70 cm in diameter for those with a rectangular field of view. They are available in various thicknesses ranging from 0.9 to 1.2 cm and are utilized in several single-headed and double-headed systems. The dimension of the crystal defines, in part, the patient area viewed in a single image. The crystal thickness affects many performance characteristics, specifically sensitivity and spatial resolution. However, its sensitivity parameter is particularly decreased for photon energies beyond 140 KeV, as can be seen in figure 10. In general utilization, a size of 0.95 cm of thickness is usually selected. Thus, augmenting the thickness of a crystal raises the probability of the total intake of ɣ-rays and the sensitivity of the detector.

For a crystal thickness of in order of 0.9 cm, in nearly 99 % of photons of ^{99m}Tc at 140 KeV that penetrate into the crystal are absorbed. The majority is absorbed by photoelectric effect, deposing thus all the energy of the photon to the immediate vicinity of the interaction point. The other part interacts by Compton effect scattering, releasing only some of the energy of the photon to the vicinity of the interaction point. The scattered photon can escape from the crystal or distribute with all of the incident energy onto several distant sites from each other in the crystal and leads thus to several light emission sites for a single incident photon [62, 63].

2.6.3 Detection Efficiency

Figure 2.10 shows photopeak detection efficiency according to incident ɣ-rays energy for scintillators NaI(TI) of various thicknesses. The gamma cameras are practically 99 % efficient for energies up nearly 100 KeV for all crystal thickness, however it shows that at energies higher than 100 KeV, the efficiency decreases according to the crystal thickness. ɣ energy of ^{99m}Tc (at 140 KeV), the difference in efficiency between 0.64 cm and 0.12 cm thick crystal is nearly 20% and the photo-

peak detection efficiency is within the range of 70% to 90%. At nearly 500 KeV, the standard ɣ-camera (a crystal thickness of 0.64 to 0.95 cm) is less than 20% efficient at transforming incident ɣ-rays into photo-peak pulses.

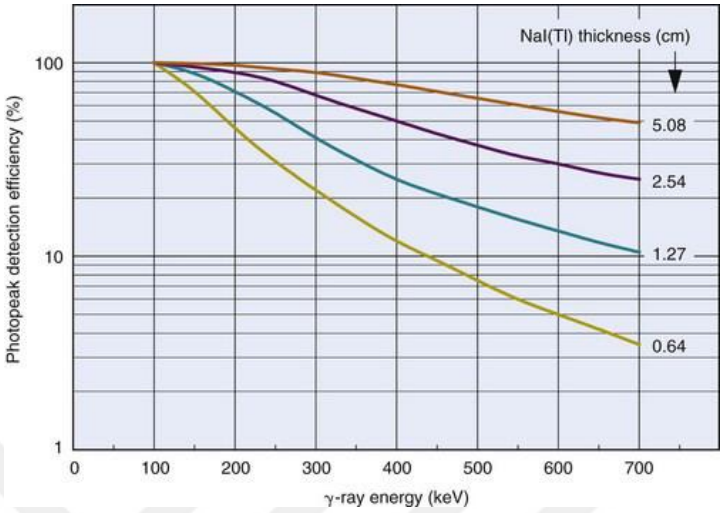

Figure 2.10 Photo-peak detection efficiency versus ɣ-ray energy for NaI(TI)[64].

2.6.4 Photomultiplier

The PMT not only transforms light into an electronic signal, but as its name indicates, amplifies the electronic signal (by a factor of 10^7) to provide a largely important current for the following electronics. The objective of the photomultiplier is to transform the light photons in an amplified electrical signal [65]. It is a sensitive and fragile device that should not be exposed to electrical or mechanical misuse. It must not be subjected to too much light conditions beyond the design specification while in operation, because this can cause it irreparable damage.

The photomultiplier composes of sensitive photocathode at one extreme, a sequence of dynodes (mostly 10) in the middle, and an anode at the other extreme. It is inserted in a vacuum glass tube with an optical window consisted of borosilicate glass or quartz to permit large transmission of light photons to a photocathode. The PMT is connected to the back face of the scintillator with an optical cement, grease or oil, and a light guide, so as to minimize the number of totals internal reflection between the surfaces. Figure 2.11 shows, the placement of PMTs (with circular or hexagonal cross-sections) narrowly packed on the surface of a scintillation crystal. It is a hexagonal array having 7, 19, 37, 61, 91, PMTs. In a recent circular gamma camera, 37-91 PMTs are utilized. Also, the Figure 2.12 shows, the position of PMTs

closely packed on the surface of a NaI(TI) crystal without its cover, which represents a rectangular gamma camera detector. The gamma camera detector measures 50 x 15 cm, which contains 30 PMTs with 5 cm in diameter. This is an example of a digital camera, in which each of the PMT outputs is digitized individually [65].

The photocathode is a thin layer of a metal compound of cesium antimony or rubidium cesium. The photocathode is coupled electrically to a series of dynodes which are set at an augmenting electrical potential. The dynode is consisted of a material like that of the photocathode and is placed at an augmenting distance from the photocathode and offset, from each other. The last dynode is well-known as the anode and is put at the highest positive potential of all dynodes in the chain.

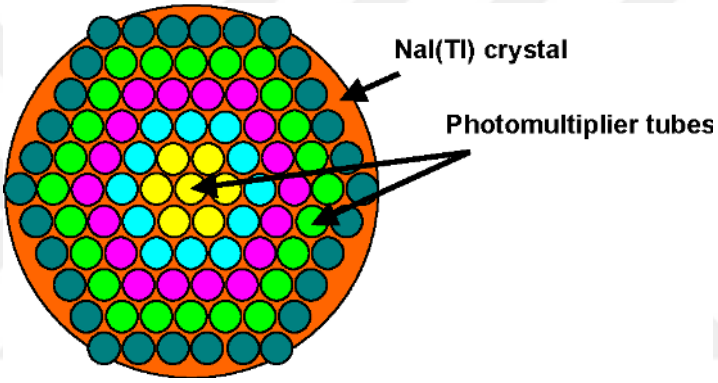

Figure 2.11 PMTs nearly packed on the surface of a NaI(TI) crystal.

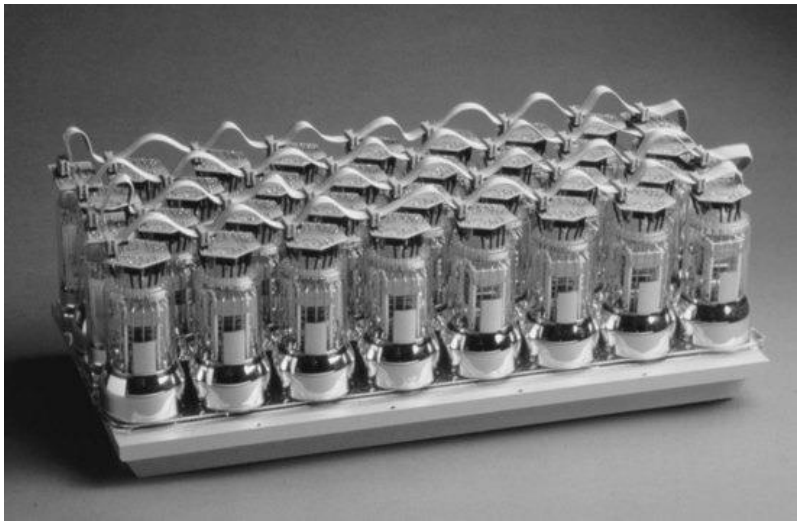

Figure 2.12 PMTs hexagonally close arranged on the NaI(Tl) crystal.

2.6.5 The Operation of the PMT

Once the light photons from the scintillator interact with photocathode, photoelectrons will be produced by photoelectric effect. The energy produced by photoelectrons is reliant upon the associated wavelength of the light photons and not the number of light photons striking the photocathode. However, the number of the photoelectrons liberated is proportioned to the intensity of light lighting the photocathode surface. The material of the photocathode presents a certain electromagnetic frequency level by which no photoelectrons can be emitted. Beyond this threshold frequency, each photoelectron liberated is capable to assume an energy that is linked to the associated energy (frequency) of light photons. Hence the spectral response of the scintillator and photocathode has to be conformed to attain a great conversion ratio.

As the photoelectrons have a negative charge, they will be accelerated to the prime dynode by an electrical field gradient between the photocathode and anode. In the process of the acceleration, the electron acquires energy, and the field gradient should be large enough thus the electrons will have strong enough energy to force out secondary electrons from the dynode surface when on effect. These electrons (secondary electrons) are accelerated in the local field between the prime and the second dynodes, and more electrons are produced at the second dynode surface. This process pursues all long of the dynode chain, till in due course there may be 10^6 times as many electrons at the anode as those commenced from the photocathode, as can be seen in Figure 2.13. As a flux of electrons constitutes an electrical current the rapid overflow of electrons can be transformed into a pulse by the applying of load resistor. The analog pulse is presented in the shape of a time varying voltage. The gain of a PMT is controlled by the number of stages in the dynode chain and the applied high voltage.

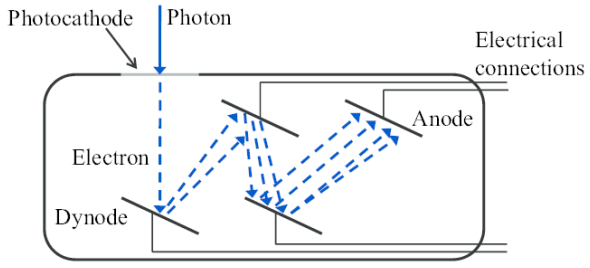

Figure 2.13 A schematic diagram of a PMT [66].

2.6.6 The Characteristics of the Output Signal

The number of light photons produced within the scintillator is proportional to the energy which is deposited within the crystal by the ɣ photons. In a similar way, the number of photoelectrons produced in the photocathode is relative to the number of light photons generated by the scintillator. Moreover, the amplitude (voltage) of the pulse at the anode is relative to the number of photoelectrons accelerated to the first dynode. Thus the result of the out voltage is relatively proportional to the energy of the interacting gamma photons.

Unfortunately, whether the signal of a scintillation detector is subjected to a source of radiation monochromatic energy is considered, there is a variation in the result of the out voltage. This fluctuation in voltage is owing to the recording of scattered ɣ photons in the scintillator and the statistical phenomena of the physical occurrences taking place in the scintillator and PMT.

The scintillation produces a spectrum of light photons with slightly variable energy pursuant to the passage taken from the conduction band (CB). This spectrum is the property of the scintillator crystal and to the nature of the impurity given (added). The number of photoelectrons produced in the photocathode relies on the geometrical source in the scintillator and the location of effect on the photocathode. The photoelectrons are likewise speeded up by changing degrees pursuant to the local field intensity which is spatially uniform.

These haphazard variations will be further multiplied on successive dynode stages. Therefore, for a corresponding complete absorption (or photoelectric) occurrences there is an outspread of output voltages around an average which amount to the mean pulse height for that specific energy interaction. To avoid more outspread of output voltages and thus acquire good energy resolution it is much relevant to utilize a stabilized HV supply.

The way passed by electrons can be acted upon by magnetic fields. So as to allow the electrons to be speeded up in a uniform path, whether is important to envelop (encase) each PMT in a metal shield which decreases the influences of errant magnetic fields.

The length time of the last pulse is basically a function of the scintillator but likewise to a lesser extent the PMT. The decrease time of the major component of the light output from NaI(TI) detector is 230 nanosecond while the increase time for a pulse in a PMT is typically 15 nanosecond. These elements (factors) and the dead time in the electronic circuits restrict the count rate and adequate spatial placing of occurrences (events) within a ɣ-camera [65, 68].

2.6.7 Preamplifiers and Amplifiers

The output signal (impulsion) from each PMT is usually small in amplitude and need to be amplified prior to further processing; it is at first passed into an individual preamplifier. A preamplifier is necessitated to set the voltage of the signal shape and pair the impedance levels between the detector and subsequent components in order that the signal (impulsion) is suitably processed by the system. Therefore, the preamplifier provides a limited quantity of signal conditioning or pulse shaping. This pulse is fed in the corresponding amplifiers where a gain in the amplitudes of this pulse is attained [69].

2.6.8 Light Guide

The light guide is made of a lucite, a quartz plate or a transparent plastic has a refractive index of 1.80, which is close to that of NaI(Tl) and it is carefully shaped to meet the shape of the PM entrance window. It helps to minimize the total reflection of optical photons and light losses in the transfer of light between the two-part, which are scintillation crystal and PM, as can be seen in Figure 2.14. It also minimizes the fluctuation of light collection productivity across the face of the crystal. It serves further to keep distance away the photomultiplier so as to the photomultiplier tubes to receive a measurable light quantity [70].

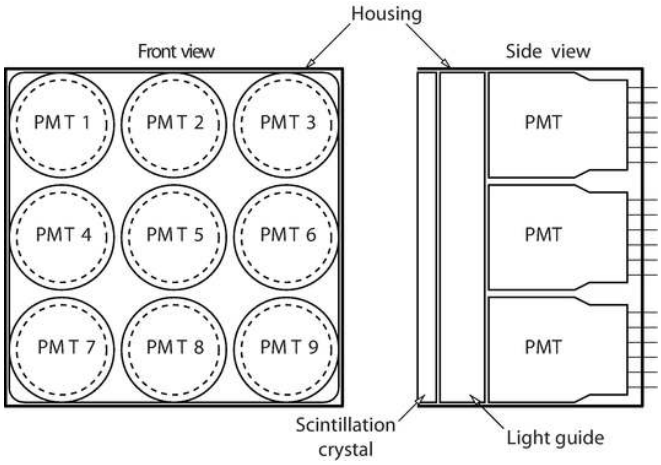

Figure 2.14 A light guide to interface the NaI(Tl) to the PMTs.

2.7 Electronic Systems

The electronic system has a main role to play which is to interconnect the photomultipliers between them and determine the localization of the energy of the incident photon in the crystal as well. The electronic system also at first permits filtering noise, by rejecting the energy of the photon gamma which is less than the threshold defined by the energy resolution of the detector. Figure 2.15 shows a photograph of the gamma camera head electronic systems which has been taken during the experimental work at GAUN Hospital.

Figure 2.15 ɣ-camera's head electronic systems at GAUN Hospital.

2.7.1 Energy Selection

To detect and measure the ɣ-rays energy, which pass through a collimator are performed as in any NaI (TI) detector system, but not the case of ɣ-cameras, which a large number of PMTs are utilized rather than a single PMT. The determination of the energy of a ɣ-ray, it needs the determination of the total number of the photon generated in the crystal. For a ɣ-camera, the total number of photons generated is distributed between many or all PM tubes. Therefore, to determine the total number of the photon generated, all photons arising from the PMTs have to add up to generate a pulse corresponding to that generated in a simple NaI (Tl) detector (with only one PMT). The added up pulse is defined as the Z pulse. PHA on Z pulses permits us to choose the pulses of the desired energy. As any other NaI (TI) detector, in ɣ-camera they exist four controls concerning the detection of the ɣ-rays and their energies: HV, amplifier gain, photo-peak energy E, and window width gamma E or % gamma E. Therefore, the selection of the energy is usually automated; to select a ɣ-ray of a specific energy, one passes a selected button and adequate pulses are automatically designated. There is also another property that provides simultaneously picking out of two or three ɣ-rays of various energies.

The sum of the signals of PM output at the vicinity of the interaction is proportional to the photon ɣ incident. To select events of certain energy therefore technically means, to select electrical signals having amplitude corresponding to this energy. The correspondence between the ɣ photon energy and the amplitude of the signal generated by the scintillation is established through a calibration. We use generally only the signals corresponding to the energy of the photo-peak [71].

2.7.2 Automatic Peak Tracking

Scintillation crystal is susceptible to slow drifts in its output, mainly owing to the variations in the gains of a PMT. Variations in the PM gain are brought about by slight ambient temperature and HV variations. In current cameras, electronic circuits have been supplied that controlling these drifts and readjust the HV or the gain of the amplifier to its initial value. The automatic peak tracking circuits track the gains of the PM either on request or continuously, relying on the manufacturer of a ɣ-camera. In either case, the PMTs output or hence the stability of the ɣ-camera itself has ameliorated significantly [71].

2.7.3 Counting

The pulses picked out by the PHA, further are sent to a circuit for production of X-Y signals (pulses), are introduced into scalar timer module. The ɣ-camera can either count for a preselected time (fixed time interval) or a preselected count (desired amount of counts). There is likewise an assistance for imaging to stop at desired time intervals (fixed time) or a fixed amount of counts, relying on which occurs first. A manual command permits to commence or stop counting at any moment. One more aspect found only in certain gamma cameras is preselection of the information density in a given zone of the image. The gamma camera will cut counting once a fixed amount of counts have been obtained in the wanted zone of the image. Gamma cameras connected with or integrated with digital computers have these functions such as number of counts, time, start, stop under computer control [71].

2.7.4 Position Determining Circuit (X, Y Coordinates)

In a ɣ-camera, a collimator permits ɣ-rays arising from a small area of an organ to get in a small area of the crystal in one to one correspondence. In order to maintain electronically this intact correspondence, one has to know the point of ɣ-rays interaction in the crystal. This is effectuated through a large number of PMTs. In this case, when light is generated at a point in the crystal, it is distributed between the PMTs. However, by distinguishing which PMT obtained the most amount of light, it is practical to get the close place (nigh the PMT obtaining the most number of light) of the point of light generation. In order to localize the point of light generation more precisely, the number of light obtained by each PMT, rather than the one obtaining the maximum light, should be considered (i.e., the light distribution between the different PMTs and hence the distribution of pulse height generated by the PMTs is taken into account).

For the old scintillation camera, the outputs arising from the amplifiers are connected to each other via a network of resistors or (capacitors) whose value is corresponded to the positions of the PMTs on the scintillator. The fluctuation in impedance and capacitance alters the signal arising from a PMT in a predefined manner and constitutes the basis of determining the coordinates of an occurrence (event). The nonlinear lattice generates a set of possible coordinate values determined by four signals: X^-, X^+, Y^- and Y^+, as can be seen in Figure 2.16, a resistive network

employed to implement position assessment. The output arises from each PMT/preamplifier is split by a resistive network with 4 outputs, X^+, X^-, Y^+, and Y^-. The correspondent signals from all of the PMTs are linked to give the summarized signal [63].

Essentially, as the signal arising from each PMT is dependent on the number of light incident on the photocathode, the location of an occurrence (event) can be done by evaluating the number of light collected by each tube pursuant to the tube position. The number of light that every tube has received demands that the total light incident upon all the tubes, owing to the same occurrence, be known. The summation of all the outputs forms the basis of a Z signal.

The pairs of signal (X^-, X^+) and (Y^-, Y^+) are added together, indeed means getting the difference, like X^- and Y^- amount to negative values, and are split up by total light output, Z, to get a signal providing the location of an event independent of the total numbers of light received. Therefore, $X= (X^+ - X^-)/Z$ and $Y= (Y^+ - Y^-)/Z$.

Thus, X and Y coordinates within the scintillator are obtained for any event. However, these signals are not perforce acceptable if the event has initiated from outside the accurate energy range.

The energy from a detected event is illustrated by the amplitude of the output pulse from the detector. Given that for each PMT output is dependent both on the geometrical relationship of the scintillation event, with the PMT, and the energy deposited in the scintillator, so the total output of the light of all the PMTs forms the energy deposited in the scintillator regardless of location.

This signal, also represented by Z, is utilized to confine the couples (pairs) of X, Y signals that match to a correct event. The Z or energy signal frees subsequent electronic circuits to the X, Y signals and may be utilized as a "strobe" to connect a chain of electronic operations. The X, Y signals amplitudes which represent the spatial coordinates of a scintillation event whilst the energy of the event is contained in the amplitude of the Z signal [72].

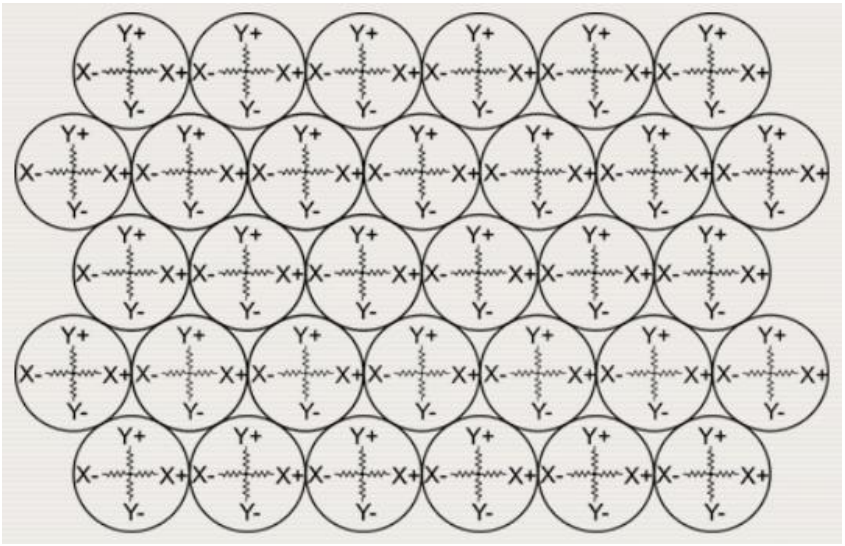

Figure 2.16 A resistive network employed to implement position assessment [63].

2.7.5 Pulse Height Analysis

The pulse generated by the amplifier can be different in amplitude due to the variation in ray energy. So, PHA is a device that selects for counting only those pulses falling within anticipated voltage amplitude intervals and dismisses all the rest, as can be seen in Figure 2.17. Furthermore, the objective of PHA is to permit the proper combinations of X, Y, and Z signals and to be processed by following image display circuits. However, the Nal(TI) crystal has a limited energy resolution when is utilized as a scintillation detector, which is usually 15-20 % at 140 KeV, and the relative predominance of little angle Compton scattered induces to the existence of far scattered radiation within the photo-peak zone: this scattered radiation is approximately 30% of the photons being scattered. The selection of an ideal window setting is a compromise between good sensitivity, which needs a large window, and a good spatial resolution, for which a small (narrow) window is good. For technetium-99, ^{99m}Tc, which is usually, recognized that for an energy window of 120-160 KeV that provides a best compromise between sensitivity and spatial resolution [73].

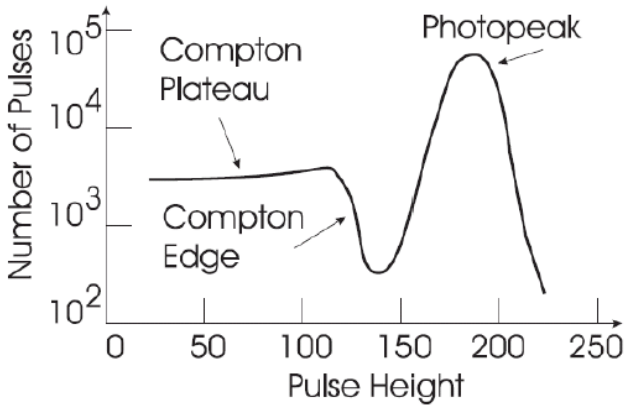

Figure 2.17 PHA circuit accepts only events fall in the photopeak (discriminator).

2.8 Image Displays

In gamma cameras, data are introduced firstly as images. As data processing by computer interconnected systems is largely utilized, conventional analog, as well as digital displays, are used. A ɣ-camera can be fitted with various sorts of image display component for the objective of imaging the radioactive concentrations while detected by the head of the camera. Ancient analog systems utilize an oscilloscope that generates an amount of light upon the CRT (Cathode Ray Tube) face at the same location on an identical X and Y coordinates system as the location of the initial interaction in the crystal or utilizes a multiformat imager that can put 1, 2, 4 or more images upon one sheet of film by a motion lens system. In digitized ɣ-camera, an image is displayed on a computer monitor. The color or the intensity at a point on the monitor being corresponded to the count of the representing pixel in the array. Certain displayers permit to change the greyscale, brightness, or contrast of the display without changing the real image data [74].

2.8.1 Analogue Displays

The most largely utilized analog display is the CRT display of a ɣ-camera. The analog signals of coordinate X and Y, matching to the position of the scintillation, are employed to the deflection plate of the tube; whether the energy of the Z signal of the occurrence is accepted by the PHA, an unblanck signal activates (switches on) the beam for a few microseconds. Each gamma being detected hence looms as a flash of light on the tube face and a continuous image is generated by incorporating these flashes on a photographic film. The principle issue with this sort of display is selecting the proper exposure for the film. The exposition will rely on the brightness

of the beam, the image count density as well as the sort of the registration film utilized [74].

2.8.2 Digital Display

The analog signals of the coordinate have to be digitalized when the image data are to be handled through a computer interconnected with display system so that the image shows as a regular array of picture items or pixels. Image intensity, the number of counts per pixel, is given by either a range of grey shades colors. The digital display gives many advantages over the analog. Particularly, given that the image is not volatile it can be handled before viewing by, for instance, modifying contrast and limiting undesirable background counts, it likewise allows quantitative information to be generated as well as advanced forms of image processing. The drawback of this sort of display is that the image may be deteriorated by the digitalization of spatial and intensity information [74].

2.9 Electronics of Modern Camera

The emergence of rapid electronic microprocessors has brought about substantial changes in the gamma camera. Output signals of the PMT are digitized rather than traveling via the resistor matrix like in Anger's camera design. This permits the sum and position circuit to be digitized as well, in a way that the position of an event can be determined through a software algorithm or lookup table. Also in most cameras, the necessary corrections are carried out numerically to make up for nonuniformity response of PMT. Also, corrections required to ameliorate image uniformity are active (applied) digitally. Digitization of the X and Y signals are joined correctly with the creation of an image within a computer matrix. Every feature of the recent ɣ-camera is controlled by a computer, permitting the operator to pick out the running time for study acquisition, or the number of counts wanted to be acquired, to set the PHA to dismiss scattered radiation, control the detector and the positions of the patient bed for SPECT and whole-body procedures, and display the image [75].

Furthermore, in modern ɣ-camera, the outputs of PMTs are amplified and digitized individually with an ADC, as can be seen in Figure 2.18. The determination of the X and Y locations of each event in the NaI(Tl) crystal is performed from the digitized signals, as it takes place, by utilizing weighted the average signals. The ɣ-ray energy, E, deposited is proportional to the all computed pulse amplitude, likewise is

calculated by adding up the individual PMTs signals. Then, if the ɣ energy, E, corresponds to the selected energy window (the range of energies to be accepted by the ɣ-camera), it is accepted and the value of X-Y signals are binned into a discrete 2D array of image elements, or pixels.

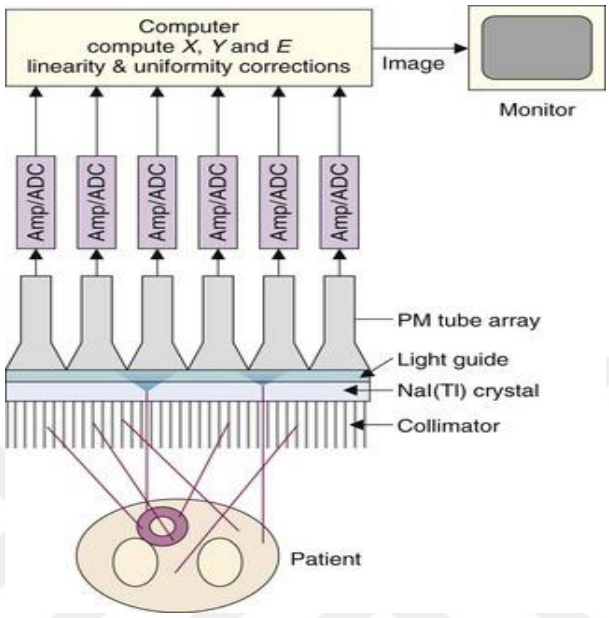

Figure 2.18 Diagram of modern ɣ-camera [76].

2.9.1 Interfacing with a Computer or All-digital Camera

The evolution of digital computers has brought a lot of advantages to NM and plays a significant role in image formations. The basic benefit of a computer is the speed and the facility in acquiring, analyzing, storing, and displaying more quantity of data. Actually, ɣ-camera can be totally integrated with a digital computer or interconnected with a devoted digital computer are available in the market. Additionally SPECT and heart studies, this cannot be carried out without a digital computer.

The analog image data generated by the ɣ-camera made up of three signals which of X and Y composing the location of the photon interaction within the crystal, and the energy signal, Z, which represents the interaction energy corresponding to the PHA energy window range defined for the radionuclide in employ. If the ɣ-camera is an all-digital one, the image information may be sent to the computer via a direct digital interface [77].

2.9.2 Digitization in General

A digital computer processes data in digitized or discrete form only and these too in binary form (i.e., utilizing only the two digits: 1 and 0; based 2 instead of base 10). Therefore, any device from which information is to be obtained and analyzed through a digital computer in an automatic way should introduce the information to the computer in digital form. Unfortunately, most electronic devices generate data or signals in an analog form. Such a device, which is able to transform automatically the analog signals into binary (digital signals), is well-known as an ADC (Analogue-to-Digital Converter). It has two relevant characteristics, which are speed and accuracy. Precision of ADC provides how approximate the digit data is to the analog signal. The more an ADC is rapid the more high rate of data and it can digitize free of any loss of information. Therefore, accuracy and speed are inversely related. The more speed the less accuracy and the more accuracy the less speed.

2.9.3 Digitization in the Scintillation Camera

In nuclear medicine, radiation detectors generate analog signals, for instance, light generated in a scintillator or pulse height generated by a PMT. Thus, all analog signals should be digitized prior to getting into a computer. In a ɣ-camera, except it is an entirely digital ɣ-camera, in which case the digitization has been already effectuated at the PMT, the X and Y, and Z signals are analogue and should be digitized prior to being recorded by a digital computer. The ADCs employed for digitizing X and Y signals of a ɣ-camera are seven to eight bits, so that the X, Y scale are identically split into 27 = 128, 28 = 256, or 29 = 512 identical divisions, respectively. In a ɣ-camera, the high range of X or Y signals will equal the crystal diameter d. Therefore, each split of an ADC can be matched to d/128, d/256, or d/512 cm of distance, relying on whether the ADC is 7 or 8 bits. For 28 cm (an 11-inch) diameter crystal and 7-bit ADC, or for an LFOV (large field of view) of 20-inch-diameter crystal with an 8-bit ADC, this value equals about 0.2 cm. Since the intrinsic spatial resolution of a ɣ-camera is actually within the range (around 0.4 cm), higher accuracy is not demanded. For the speed of the ADC, it ought to be capable of handling about one hundred thousand signals per second since greater counts rates are rarely meet in nuclear medicine. Digitizing the signals of X, Y into 64, 128, or 256 divisions provides a 64 × 64, 128 × 128, or 256 × 256 matrices. Thus, the analog data or image (which is a 2D or planar distribution) is split into 64 × 64 = 4096, 128

× 128 = 16,384, or 256 × 256 = 65,536 represent small areas known as pixels or picture elements that are distributed in a 2D matrice. There is a particular area on the crystal which matches to a particular pixel (provided by its column and row number), and each pixel is attributed to a particular location in the computer memory. Therefore, during the interaction of a ɣ-ray in the crystal, its pixel position is established by the ADCs and a count is stored in the relative place in the computer. As more as possible ɣ-rays interact, they are stored in convenient locations, and ultimately a digitized image is made.

In digital ɣ-camera, the outputs from the ADC are usually performed in two modes during data acquisition by the computers, which are the list and frame modes. In list mode, the digital information describing the coordinates of the interaction of photons within the crystal are merely stored as lists in memory. In contrast, in frame mode, the digital information are utilized to establish the address of a particular memory position matching to the position of the interaction [78, 80].

Figure 2.19 shows a simple graphical example of digitization of an image generated by a ɣ-camera, utilizing a 4 × 4 matrix consisting of 16 pixels. In this example presented here, the X and Y ranges are each split into 4 divisions, resultant 4 × 4 matrix has 16 pixels and has a poor spatial resolution. Thus, to obtain a good spatial resolution, the analog image generated by a ɣ-camera is split into a number of square cells or pixels (64 × 64 = 4,096, 128 × 128 = 16,384, or 256 × 256 = 65,536, which are utilized in practice). Counts from each pixel are stored in a part in a location in a computer [81].

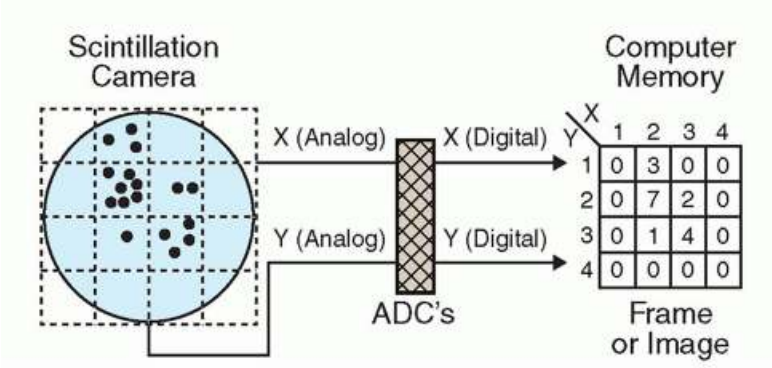

Figure 2.19 Digitization of an image generated by a ɣ-camera.

2.10 The largest Modalities of Scintigraphic Image Acquisition

The gamma camera can be used in several ways in terms of acquisition modes. It typically depends upon the organ to be explored and the pathology to be identified. These different types of operations used by a gamma camera are called acquisition modes which are executed either in planar mode or in tomographic mode [82].

In planar mode, the image corresponds to an acquisition under a single incidence. It is therefore a projection of the structure being examined. It thus explores only the part of the body facing the detector's field of view.

In tomographic mode, the detection heads of the gamma camera are rotated around the patient, the image is then being reconstructed from projections taken under different angles of incidence.

2.10.1 Static Planar Acquisitions

The acquisition heads are in an immobile position relative to the target (patient). It is interested here in the distribution of the radiotracer when it is fixed relatively stable into the organism. The recording is interrupted after a predefined time (pre-time mode) or after the detection of a predefined number of photons (pre-count mode). It is applied for the examination of kidney, thyroid. Figure 2.20 shows an image of thyroid, in static planar mode imaging [82].

Figure 2.20 Static planar mode imaging.

2.10.2 Dynamic Planar Acquisitions

The acquisition detectors (heads) are in a fixed position. A number of images are successively acquired, at the rate of a few seconds per image: the acquisition as a

function of time. It is used to examine certain interesting dynamic biological processes. It is applied to study as kidney and bone phase's vascular scans and scintigraphy of the heart ventricle. It is also used for knowing the kinetic of the tracer (fixation speed or elimination of the tracer within the organ of interest).

2.10.3 Gated Planar Acquisitions

Gated acquisitions are used for cardiac scintigraphy studies. During these acquisitions, heads (detectors) are fixed in the form of an "L" and at the same time register the radioactivity from myocardium and the electrical activity of the heart. These acquisitions are similar to the dynamic planar acquisition, but they commence at a particular point in the cardiac cycle, usually acquired during each cycle. Thus, these acquisitions are synchronized by the heartbeat cycle which is registered by the use of ECG electrodes, as can be seen in Figure 2.21 [82].

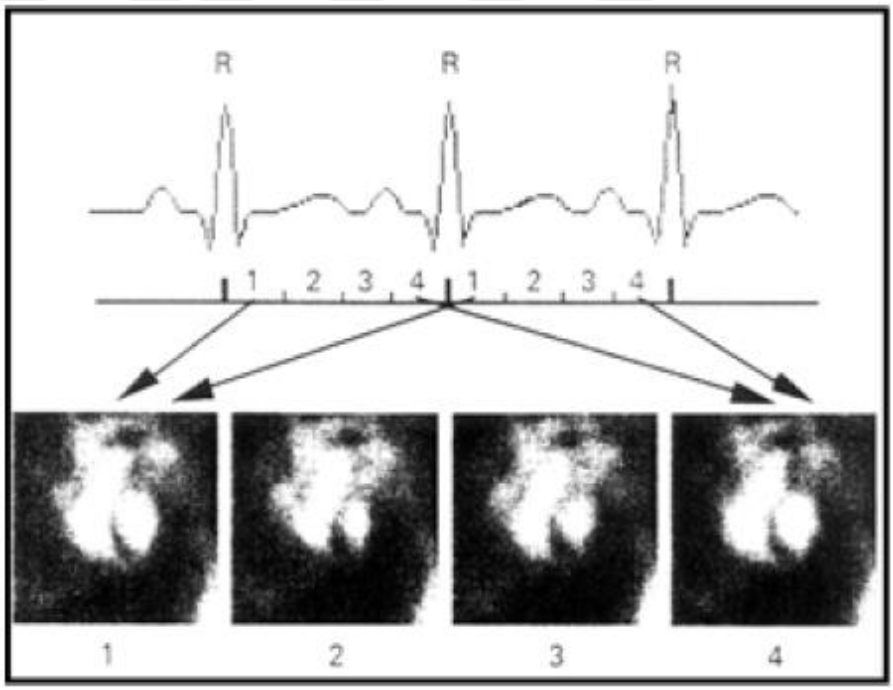

Figure 2.21 Synchronized acquisitions with ECG.

2.10.4 Tomographic Acquisitions

Tomographic acquisitions are used by SPECT. In this application, the acquisition heads (detectors) are rotated around the patient; several images are successively acquired, at a different angle. Obtain the representation of the radioactive distribution of the body in 3D. It is used to study the chest, pelvis, and skull.

2.10.5 Synchronized Tomographic Acquisitions

Similar as to simple tomographic acquisition, the detectors are rotated around the patient. Under each angle of view, synchronized acquisitions are realized with heartbeat cycle. We thus obtain the radioactive distribution representation in 3D, during the heartbeat cycle.

Besides, a particular acquisition is whole-body scan, as shown in Figure 2.22, succession of static images linked. Due to the size of detector surface is smaller than the whole body, it is necessary to move the detector so that can scan simultaneously the patient's whole body from head to foot. This acquisition is used to study for metastases, which are cancer cells that can migrate in the body from a primary tumor [82].

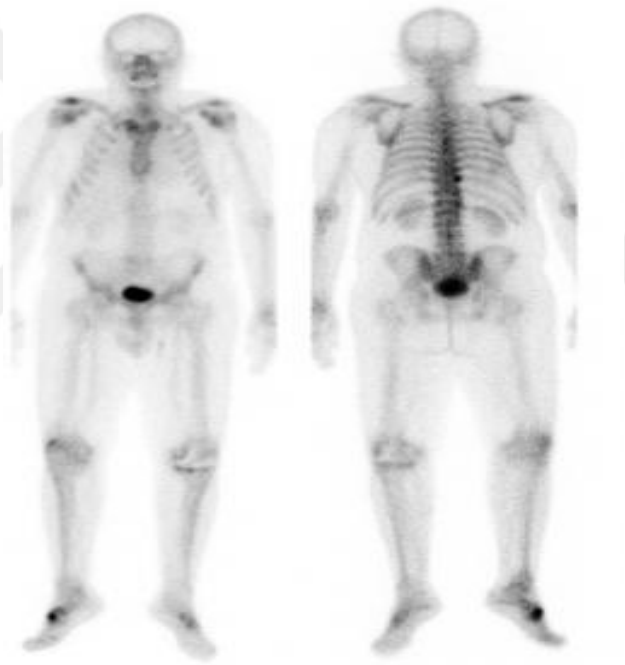

Figure 2.22 Whole-body scan by SPECT imaging.

In all acquisition cases, the patient must be motionless; otherwise, the images will be blurred. Also, the choice of acquisition type depends on among other things upon the organ of interest or studied.

In similar way as it is can be carried out in X-ray imaging, a simple radiography or a scanner, a planar acquisition or a tomographic acquisition can be realized in scintigraphy. Planar acquisition is pointed out when concerning the depth details is not indispensable, for instance, when is interesting in skeleton or to the joints (hence

their thickness is small and there often is no fixing structure importantly, the radio-tracer is superposed at the skeleton). However, in a planar acquisition, structures located at different depths are projected on the same image area and we cannot separate them. On the other hand, it is impossible to determine in the organ of considerable thickness (for example, the brain), at which depth located the organ of interest. To know the depth, the tomographic acquisition that allows obtaining slices (sections) of the body is required.

2.11 Attenuation and Scattered Corrections

2.11.1 Attenuation Corrections

Attenuation of gamma photons is an exponential function proportional to the thickness of the tissue to be penetrated (crossed) by the photons which interacting in the medium and causes image artifacts. Thus, free of attenuation correction, the structures will see their activity as much underestimated as they are deep. Correcting this attenuation, it is necessary for each pixel, and under every coincidence, knowing the thickness and the attenuating nature of the tissue crossed, in other word, it is necessary to arrange tissues attenuation map. Various methods are employed for the determination of the attenuation map. It can be obtained by the X scanner, which is naturally adapted to the measure of attenuation, but then technically delicate problem arises of registration in 3D space, scintigraphy, and images of the scanner.

Another great approach consists to use a uniform attenuation map, i.e. which all coefficients are identical for all tissues. The correction applied to a pixel then depends on its depth. This approach is rather used for structures which are relatively homogeneous in term of attenuation, in particular, the brain. Uniform correction method is not adapted to the tomographies performed on trunk, owing to the diversity of the large structures in terms of attenuation (bone, soft tissue, pulmonary air, etc.). That is why some systems have been proposed for some time, to realize an attenuation map with the help of an external radioactive source. These systems are mounted on the gamma cameras, the subject is located between the source and the detector, as in an X scanner. It is also realized on all projection angles, a series of "attenuated" projections which is used to construct cross-section images of the attenuation. One of the solutions consist of a machine with two heads placed at right angle, to simultaneously acquire on one of them, the photons transmitted by the

external point source and the photons emitted by the radiopharmaceutical in the body, and on the other, to acquire the photons emitted by the radiopharmaceutical alone. A fan-beam collimator is useful when using a point source.

2.11.2 Scattered Corrections

Scattering of Compton effect is the phenomena at which during a gamma photon is deviated from its path by passing near to an electron loses part of its energy. A scattered photon which attains the detector provides erroneous information. If the scattering phenomenon is significant, it can make the image blurred. They exist several methods for scattering correction. The method applied by all gamma cameras consists of only considering photons whose energy is close (neighbor) to that of the photo-peak. Indeed, energy with a lower that of the photo-peak, which means it has been considered as scattered photon. Unfortunately, the limited resolution in energy of detectors does not permit us to distinguish perfectly the primary photons (not scattered, but whose measured energy does not always of that the photo-peak because of the measure system imprecision) and the scattered photons. It therefore is necessary to distinguish the non deviated photons in the photo-peak window. One solution consists of simultaneously acquiring images at several energies that including the photo-peak energy. The scattered present in the photo-peak window is then estimated by more or less complex algorithms, then is totally subtracted from the image to get an image with less scattered. There is no currently perfect solution for scattered correction [83, 84].

CHAPTER III

QUALITY CONTROL OF GAMMA CAMERAS

The gamma cameras are the most largely utilized diagnostic imaging system available in nuclear medicine departments. Due to their physical characteristics, gamma cameras need very careful attention and, thus, more regular and numerous tests than any other diagnostic imaging technique (modality) in radiology.

It is largely acknowledged that the achievement of great levels of efficiency, quality, and accuracy in the practice of NM, as in other fields based on high technology, needs a suitable quality control program. The basic safety standards published by IAEA reported that all instrument or equipment employed in NM for study or medical care purposes should be exposing to internal QC [85]. Quality control test has a significant, sensitive role in checking variations in performance so as to service can be planned and carried out prior to the necessity becomes crucial and demands annulment of patients examinations. Also, the regular assessment of QC is performed in purpose to detect or prevent variations in the performance of a ɣ-camera system that may be unfavorably affecting the analysis of clinical studies. Moreover, on a daily basis, there is a restricted amount of time that can be reasonably dedicated to system QC. Therefore, the main objective of a quality control program has to control those parameters that are: The most sensitive to changes in system performance and the most susceptible to affect clinical studies. Obviously, there are a large number of factors that participate in the final image quality, such as uniformity, intrinsic resolution, energy resolution, collimator, and hard copy device. Besides, for some types of studies, other factors, including count rate or sensitivity ability come into play. So, the success of each quality control program required various types of imaging phantoms, which are may be constructed from acrylic containers filled with liquids containing radionuclides. These phantoms are utilized to test the performance characteristics of the ɣ-camera. They are also utilized to measure radiation dosage,

for teaching objectives, to calibrate equipment and for research and they are utilized to demonstrate to researchers and technicians the relationship between the physical object scanned and the final image. They are a fundamental part of keeping great diagnostic QC and assurance. Thus, this study will focus on certain of the more crucial areas in QC of ɣ-camera systems, such as uniformity, linearity, spatial resolution, and contrast using an in-house phantom.

3.1 Why Quality Control?

Evaluation of the performance of an instrument is of uppermost importance, it is not just during the time of the installation, but likewise at constant periods during its utilization, especially after major repairs [86, 87]. Quality control assessments at a regular period are further of great help in detecting degradation in the performance characteristics of an instrument as it gets older. At first, upon accomplishment of installation, it is paramount importance to assess and record optimal performance parameters of the instrument as a baseline for future reference. When lying down these baseline parameters, protocols have to be developed that can be carried out with accessible in-house facilities and can be accomplished in a reasonable time. The requirement for quality control tests for acceptance during the time of installation and for later follow-up during the time of its utilization is much more substantial in developing countries because of the changes in the performance engendered by frequent variations in temperature, humidity, and power supply. Besides, the technical or support service and maintenance access in a developing country may be either destitute or at times nonexistent.

Briefly, quality control is primordial at acceptance level, at the time of routine operation as a control on maintenance measures, and for inter-comparison of various systems.

There are exist several organizations that have established quality control procedures and protocols for the gamma camera, we can mention some of them:

-AAPM: American Association of Physicists in Medicine,

- IEC: International Electrotechnical Commission,

-IAEA: International Atomic Energy Agency,

- NEMA: National Electrical Manufacture Association.

During this work, it was much more based on the procedure of NEMA standard which is the most commonly employed procedure.

3.2 Principles of Quality Control of Instruments

To carry out quality control tests in practice, employing quality control phantoms or test objects, on scintillation camera, it is necessary to be already informal with the general principles of a planar and tomographic ɣ-camera system, as imaging apparatus utilized in nuclear medicine. Simply, planar ɣ-camera systems provide 2D images, whereas tomographic ɣ-camera systems provide a 3D image, which is known as SPECT.

A basic principle in the QC of a ɣ-camera in nuclear medicine is that it must be taken on as an essential part of the task of the nuclear medicine service and by the staff of the service members themselves. Therefore, certain aspects should be handled in coactions with the maintenance team. Figure 3.1 shows a diagram of QC program.
The QC of each device must have as its commencing-point, the selection and acquisition of the device itself, given that devices can be widely different in their performance. The selection of an adequate site for installation of the device must be as well taken into consideration within the aspect of QC, insofar as it may affect performances. After its reception and installation, the instrument must be subjected to a series of acceptance tests conceived to determine if its original performance complies with the specifications of the manufacturer. Simultaneously, reference testing has to be performed to supply data from which its ulterior performance may be carried out by routine on daily basis tests, weekly, monthly, quarterly, yearly. Lastly, operational controls, performed daily the instrument is utilized, must be applied in vigor. Attentive records of the outcomes of all these tests have to be preserved and, whether these show undesirable performance, proper corrective measures should proceed. These QC procedures do not, of course, prevent the necessity for regular preventive maintenance procedures, which should still be performed regularly.

The achievement of such a program relies predominately on its comprehensive and acceptance by all implicated. It further needs an evident determination of responsibilities, rigorous adherence to test schedules and protocols, and real establishments for the monitoring of test outcomes [85-88].

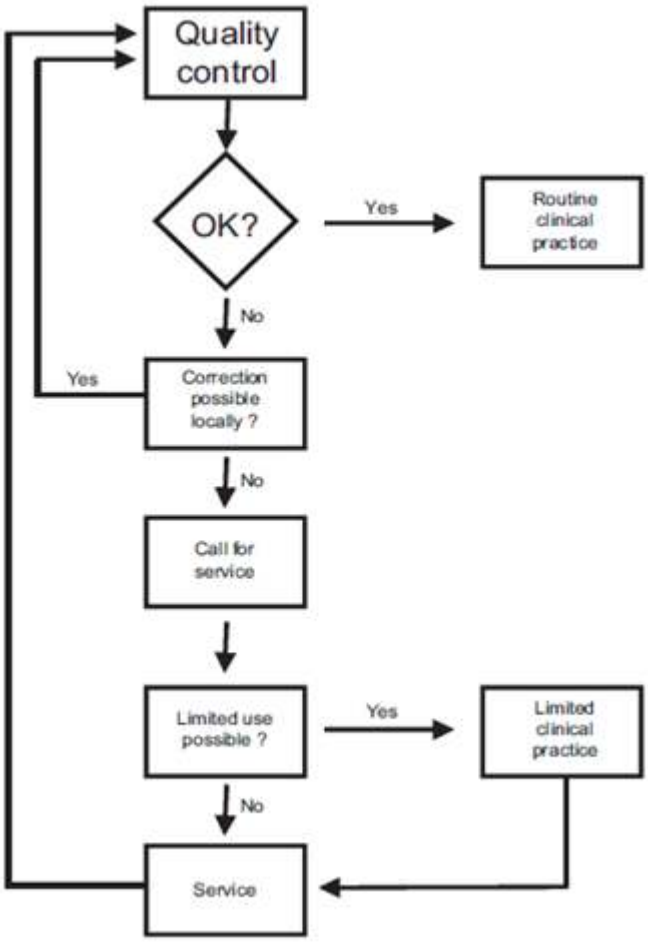

Figure 3.1 Diagram of a QC program for a ɣ-camera [85].

3.3 Phase and Content of Quality Control

The life cycle of nuclear medicine instrument is scheduled starting from the intention to procure and terminating at the disposal of the equipment, which includes tests conducted at the time of the working life cycle of the equipment. Quality control tests are performed during the acceptance testing and clinical usage of the equipment. Also, because of the sophistication and susceptibility of NM imaging instruments, absolute care and effort have to be paid to preventive actions and operation of radiation detectors, including cares, manipulations, and protections versus the main environmental conditions follow:

- Establishing a suitable protection program must provide efficient humidity, AC (Air Conditioning), dust, and pollution control, etc (i.e., climatic environmental of the instruments),
- An appropriate protection program that has to provide proper AC line power conditioning versus lightning, power line perturbations, electrostatic

discharge, and electromagnetic interference. The employ of a non-interruptible power supply is recommended to keep safe the system from the occurrence of power defeat (i.e., electrical environment of the instruments),

- A proper preventive scheme ought to provide well-timed training of the machinists, technicians, and service engineers on the proper employ and assurance of the devices. In order to cope with the service and maintenance of sophisticated NM equipment, specifically qualified and skilled service personnel has to be permitted (i.e., human environment of the instruments),
- NM device is subtle to magnetic field and must not be installed near to MRI (Magnetic Resonance Imaging) scanners or other highly magnetic machines (i.e., magnetic environment of the instruments),
- Adequate protection must be taken into consideration, at the time of scheduling and installation, the site of significant radiation sources, for instance, PET facilities, X-ray machines, ^{60}Co devices radiotherapy, and linear accelerators. NM devices are strongly sensible to these extreme energy sources and should be installed at adequate locations from them. It is recommended to keep off place of radio-pharmacy facilities near to the imaging rooms without neat attention to shielding. The storage and displacement of radioactivity materials, patient as well, in the surroundings of NM instruments ought to be also avoided (i.e., background radiation).

It must that all these preventive actions be correctly assumed before the installation and remains to be kept at the time of operation till disposal from service of the instrument, conforming to current safety standards.

It is extremely significant that all directives provided in the operation manual and service manual for adequate manipulation of the device have to be neatly pursued and that all the requirements of the manufacturer for the protection have to correctly conform prior to its installation [85-91].

3.4 Acceptance and Reference Testing

Acceptance performing of a device subsequent its reception and installation is a crucial point towards the attainment of great quality performance, and ought to be undergone to consequently attentive testing. Acceptance testing is taken on to make sure that the performance of a machine conforms to the technical and performance

specifications cited by the manufacturer. It ought to be performed instantly subsequent installation in order that the provider can be briefed of any damage, imperfections, or deficiencies before the guarantee has expired. No machine ought to be put into use, except it has been demonstrated by acceptance testing to be carried out optimally. A device that doesn't carry out properly at installation has a high probability of never doing so.

Acceptance tests are carried out to check that the instrument carries out according to clearly to its specifications. All instruments are provided with a set of fundamental specifications. These are produced by the manufacturer under standard test procedures, which ought to be traceable to standard protocols, such as IEC and NEMA performance standards. By following these standard procedures within clinical context, with help from the seller providing the software and phantoms where needed, specifications can be tested. Certain acceptance tests are basic performance tests that ought to be redone on either a periodic or a routine basis, and these acceptance tests supply reference data that the customer can refer to next time the whole life of the system. Besides acceptance tests that check specifications, further tests are mostly needed at acceptance so as to more rigorously test individual components of an instrument, and these are invoked to here as reference tests. These reference tests may unfold a problem with performance that requires to be rectified by the manufacturer prior to the system is accepted. Certain reference tests are simpler models of the acceptance tests, utilizing phantom tools disposal in the department. The outcomes of each test performed at acceptance develop the guideline reference data for any future quality control tests. These acceptance test results from the reference data for future quality control tests and some may be repeated periodically, such as at half-yearly or yearly intervals, or whenever a major service or component change has been carried out [85].

3.4.1 Routine Test

After the instrument has been accepted for clinical practice, its performance requires to be checked routinely with straightforward QC procedures that are vulnerable to variations in performance. These tests should be carried out by suitably qualified and trained staff, and comprehensive local operating procedures ought to be recorded for this routine task. Each test outcome should be written and verified for changes, and

proper measures carried when variations are detected. The quality control tests are a major part of the routine work, and enough equipment time and staff time should be attributed to routine QC.

3.4.2 Recordkeeping

Record keeping of QC and ordered registering of the outcomes of such procedures are necessities of a compliant QC. Recorded details of all most important QC procedures, comprising the acceptance limits of the outcomes of each such procedure and the corrective measure for an out of tolerance outcome, must be involved in the procedure handbook of the setup; for each procedure, the recorded description must be dated and signed by the establishment director, physicist, or other responsible individuals. In all quality control test carried out, the initials data and following data, must be written on an organized and appropriately interpreted form: the performed test; the time of the test and date; the mark, model, and serial number of the device tested; the outcomes of the test; and a notation showing whether the test result was or was not within the acceptance range. These records must be kept in an orderly way in a safe (i.e. chronologic) and in an easily accessible place. It is usually useful to follow the outcomes of quality control tests in the form of a graph of the digital result with respect to the date of the test. In this manner, long-run trends in equipment performance, oftentimes inappreciable form one day to the next, can become evident. More and more, these records are conserved in electronic form or are computerized. Also, records should still be kept in hard-copy form and it is suggested to do so in every case, both like a backup and for practical review by controllers and other inspectors [92, 92].

3.5 Preventive and Corrective Maintenance

The significant maintenance procedures performed on an instrument by maintenance staff of the manufacturer's representative and its quality control and straightforward by the staff of the nuclear medicine unit ought to be seen as supplementary to each other. Maintenance procedures are performed on purpose to keep an instrument in the best practical working condition, but they cannot ensure that it carries on so, nor that it is utilized properly in a given procedure.

Constant preventive maintenance is crucial to the ongoing adequate performance of each instrument. Straightforward cleaning is needed to keep it outwardly impeccable

and inwardly without dust and dirt. Moving parts should be lubricated and short-lived components substituted. Systematic careful examinations are essential to detect failures, nascent, or present before they expand into significant damages. Especially relevant in the latter respect are electrical and mechanical inspections that relate to the protection of patients and staff.

Some tests utilized in QC may should be redone while preventive maintenance or subsequent corrective maintenance for the repair of a failure. It is subsequently very crucial that these tests are regularly performed according to the same protocols and their outcomes are regularly compared with the reference data.

Preventive maintenance should be regularly performed and monitored utilizing the required quality control tests. A proper maintenance program needs to include the following basic procedures:

- ✓ Quality checks of components, electronic circuits, connectors, pieces, and cabling, etc.
- ✓ Check of sensor/detector condition.
- ✓ Inspection of low and voltage power supplies.
- ✓ Preliminary setting of energy and position signals and preamplifier adjustment, etc.
- ✓ All the calibrations of the correction circuits, for instance, uniformity, linearity, energy, and attenuation, and scattered corrections.
- ✓ Checks of the integrity and normality of moving parts, by taking in consideration cause of the lifetime and usury of pieces in recurrent employ, including cables, relay switches, etc.

As in the case of corrective, preventive maintenance depends on one instrument to another. Given that, the protocols will vary from device to device. Habitually, preventive maintenance is regularly performed by qualified and skilled service engineers with contracted service. Besides, all documentation, which includes service circuit diagrams and manuals, essential test devices, and radiation sources, should be provided at the procurement stage [85].

3.6 Performance Characteristics of Gamma Camera

For the gamma camera, the most pertinent performance parameter including uniformity, spatial resolution, linearity, energy resolution, count rate, etc. This work

will present more details about uniformity and resolution parameters which are the most important performance characteristics and should be performed periodically in each department of NM [93-95].

3.6.1 Response to Uniform Irradiation (Uniformity)

Uniformity is a quantification of the degree or quality with which the ɣ-camera provides a spatial uniform ɣ-ray flux, or a uniform density, which is the outcome of variations in energy response and spatial linearity through the face of the ɣ-camera. It is crucial to evaluate such a non-uniformity since these areas, high or low-average count density can be confused with abnormal pathology in clinical images. Figure 3.2 shows the uniformity degree of the counting density in the image when the detector is irradiated by a uniform flux of photons. At 140 KeV photo-peak of ^{99m}Tc with energy window of 20%.

Flood-field uniformity may be measured as the intensity of uniformity exposed by the detector itself or by the detector with collimator attached. It may likewise be measured in terms of the maximum change in count density over the integral field of view (i.e., IU) or in terms of the maximum rate of variation in count density over a defined distance (i.e., DU). Therefore a small change or rate of variation represents to good or high uniformity. Thus, the integral and differential uniformity are expressed as follow:

$$\text{Integral Uniformity} \quad (\text{IU}) = \frac{(\text{max}-\text{min})}{(\text{max}+\text{min})} \times 100 \tag{3. 1}$$

$$\text{Differential Uniformity} \quad (\text{DU}) = \frac{(\text{max}-\text{min})}{(\text{max}+\text{min})} \times 100 \tag{3. 2}$$

The main factors that deteriorate intrinsic uniformity are the bad arrangement of the gains of PMTs (Photomultiplier Tubes), failing of one or more PMTs, spatial non-linearities, defaults in or degradation of the crystal, physical isolation of the PM-light guide set from the crystal, improper adjustment of the position or width of the PHA window, and high count rate. Further factors that deteriorate system uniformity are defects in or damage the collimator.

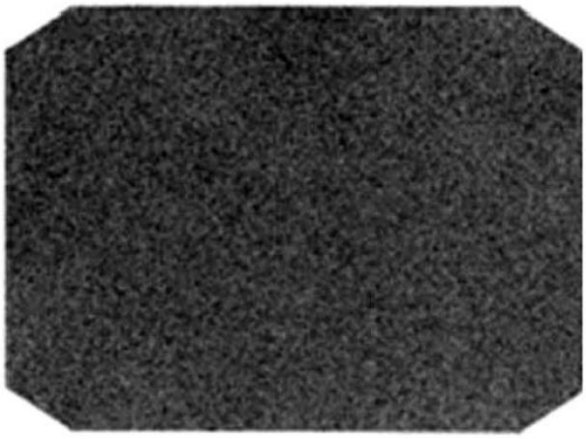

Figure 3.2 Routine uniformity test.

3.6.2 Non uniformity Response

The non uniformity describes the ability of the scintillation camera response when is irradiated with a uniform flux of photons resulting in image displays zonal fluctuations in count density. The degree of non uniformity in the flood image is sensitive to fluctuations in a number of performance parameters, as shown in Figures 3.3, 3.4, 3.5, and 3.6.

The main factors that affect intrinsic uniformity are:

- The maladjustment of the PM gains,
- The failure of one or more Photomultipliers,
- The spatial non-linearities,
- The defects or degradation of the crystal,
- The incorrect setting of the position or width of the PHA window and the high count rate,
- The electronics associated.

Other factors also can degrade the uniformity system such as defects or damage of the collimator.

The Figure 3.3 shows a defective photomultiplier. During a daily QC image test of uniformity, at 15% of the energy window of ^{99m}Tc. The image shows a large circular cold area that was because of a faulty PMT. This problem requires service [85].

Figure 3.3 Defective photomultiplier.

Figure 3.4 shows a maladjusted PM tube amplifier. During a routine uniformity control with a ^{99m}Tc at energy window 15 %, a 128 × 128 matrix. This image has been ameliorated. Hence, at the top right of the image, there is a distinct non uniformity: a hexagonal pattern characterized by two edges of raised counts. This was owing to a failure in the adjustment of a PMT [85].

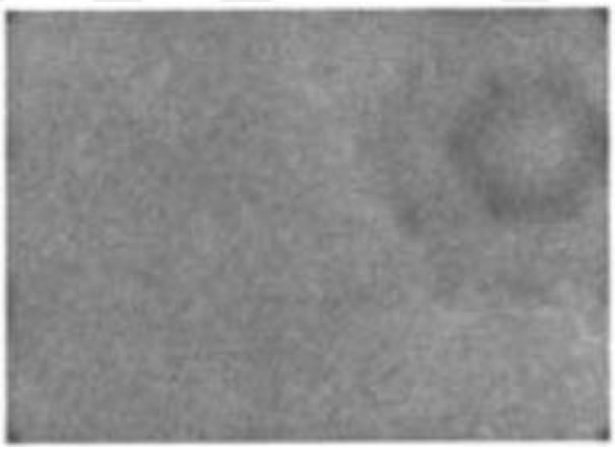

Figure 3.4 Maladjusted PM tube amplifier.

Figure 3.5 shows defective electronics associated with PMTs. During a routine quality control test of uniformity with a ^{99m}Tc at energy window 15 %. Thus, at the bottom and top of the image edges, there are three cold indentations. This is because of defective associated electronics with the PMTs [85].

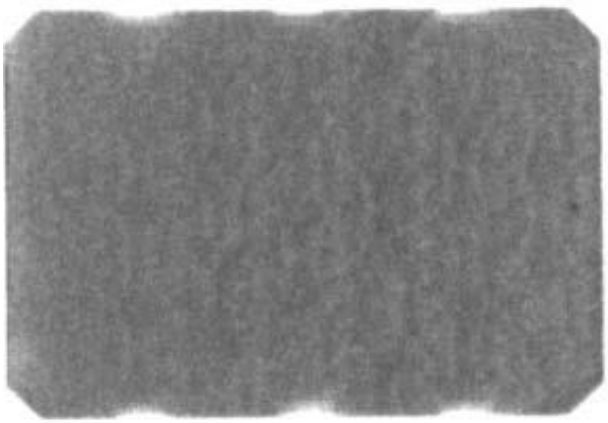

Figure 3.5 Defective electronics associated with PMTs.

Figure 3.6 shows a cracked crystal. This is revealed during a routine uniformity test that the crystal presents different cold areas with hot edges. These fissures are because of thermal variations. The hot edges are because of the reflection of the light at the fissure of the crystal [85].

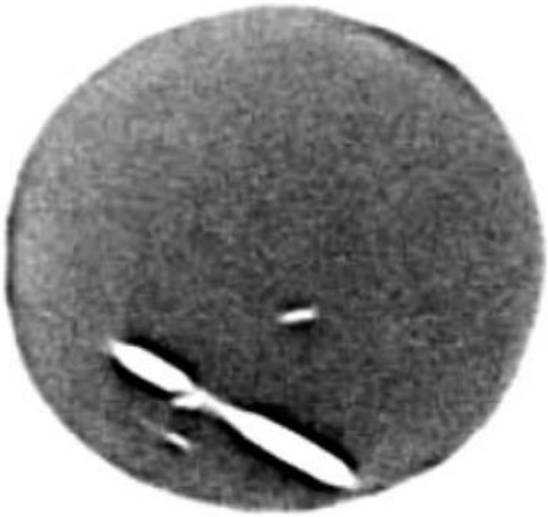

Figure 3.6 Crack crystal.

3.6.3 Spatial Resolution

Spatial resolution is a performance property of a gamma camera that qualifies its capacity to determine two separate point or line sources of radiation as distinct entities.

It is commonly measured either as the full width at half-maximum (FWHM) of the response to a narrow line source perpendicular to the long axis of the source, or as the minimum detachment of two sources that can simply be discerned from each

other. Thus, a small width or separation corresponds to good or "high" spatial resolution. The intrinsic resolution, Ri, presented by the detector itself is termed the intrinsic resolution. The collimator itself represents a spatial resolution, Rc, which is good when the source is placed at the collimator surface and becomes progressively worse when its distance between the source and the collimator augments. The system resolution, Rs, of the detector collimator attached can be evaluated for a source placed at any specified distance or interval from the collimator by:

$$R^2s = R^2i + R^2c \qquad (3.\ 3)$$

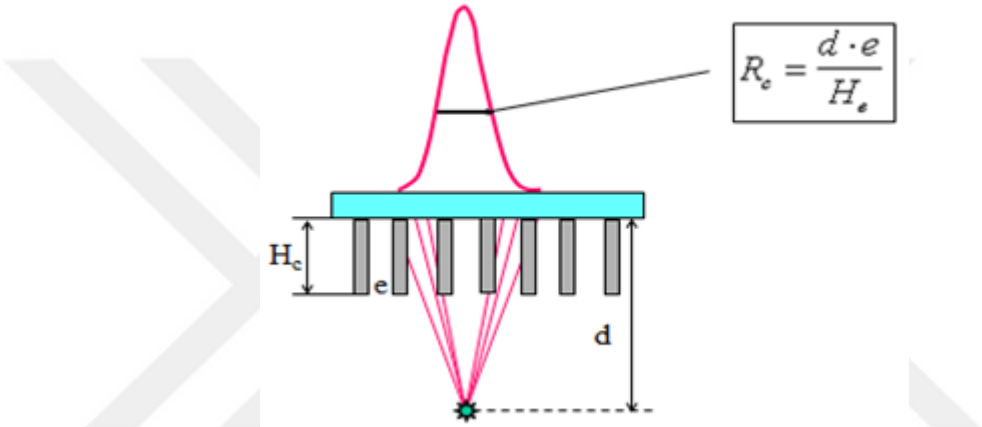

Figure 3.7 System resolution of a ɣ-camera collimator.

where e is the collimator holes diameter in mm, d is the distance between the collimator and the mid-width of the plane detection in mm, and H_c is the collimator holes height, as can be seen in Figure 3.7.

Usually, intrinsic spatial resolution ameliorates with rise in number of PMTs for the same crystal diameter or energy of entering photons, and with diminution in thickness of crystal, or width of PHA window, count rate, ratio of scattered photons, and light guide. Collimator resolution ameliorates with augmentation in the number or length of holes and diminishes in the diameter of holes or thickness of septa.

The main factors that deteriorate intrinsic spatial resolution are electronic component breakdowns, bad conjunction of PMs gains, failing in or degradation of the crystal, and high-count rate. In certain cameras, shifting to the high count-rate mode diminishes spatial resolution. System resolution is influenced by the selection of the

collimator and deteriorates while the distance between the radiation source and the surface of the collimator rises [85].

3.6.4 Spatial Linearity

It is the ability of the gamma camera to render the accurate form of an object after being imaged (without linear distortion). Spatial linearity can be determined by analyzing the level of spatial deformity or geometric distortions produced when reproducing the image of a bar or slit phantom. The spatial distortion represents the linearity degree in the image of a linear object.

Also, spatial distortion can be measured as the maximum spatial move on the field of view and may be evaluated by examining the image of a linear object. Such small deviations will cause non-uniformities in the areas of otherwise uniform count density.

The spatial distortion is closely related to the flood-field uniformity. If serious spatial shifting takes place, in the same region, the uniformity degree will be affected.

The major factors that deteriorate spatial resolution are misalignment of the gains of PMT, failing of one or more PMTs, inappropriate adjustment of the position of PHA, high count rate, damage to the collimator defects in the crystal [85].

3.6.5 Energy Resolution

It is the ɣ-camera's ability to discern the photons that have different energies and select accurately the photo-peak total absorption by photoelectric effect and thereby eliminate as much as possible the primary and scattered radiation. It usually measured as the FWHM of the photo-peak, quantified in energy units. This is provided in percentage (%) of the ɣ-radiation energy (FWHM %). Thus, a low FWHM % represents a good or high energy resolution [85].

The main factors that affect the energy resolution are:

- The misalignment of the PM gains,
- The malfunction of one or more PMs,
- The dysfunctions or degradation of the crystal,

- The physical separations of the crystal-light guide-PM assembly and a high counting rate.
- The electronics associated.

To ameliorate the overall energy resolution, most of the gamma cameras have energy correction electronic methods that align the photo-peak and generated by each PMs.

3.6.6 Sensitivity

The sensitivity of a NM imager is the factor that describes the degree of the stability of its response towards gamma radiation. By definition, it is the count rate per unit activity; with the units: cpm/μCi (counts per second per micro curie). Furthermore, it is determined by the number of photons received by the system, as a function of source activity, within the full-energy peak window. It depends on the ɣ-camera's electronic systems such as: crystal and PMT along with their characteristics, design, and performance. It can be altered by the (i) imager's geometrical profile, (ii) stopping power and depth of the detectors, (iii) radionuclide's energy, (iv) imager's energy resolution and energy window, and (v) source distribution and its position in the imager.

Furthermore, the main factors that deteriorate intrinsic sensitivity are count loss because of high count rate, misalignment of the PMs gains, malfunctions of one or more PMs, spatial non-linearities, faults in or deterioration of the crystal, physical separation of the PM-light guide assembly from the crystal, and inappropriate adjustment of the position or width of the PHA window. Besides factors that deteriorate system sensitivity are imperfections in or damage to the collimator [85].

3.7 Tests Frequency

Tables 3.1, 3.2, and 3.3 present the most important quality control tests for a gamma camera, which is based on suggestions of manufactures and standard organizations for frequency tests. Some operational controls should be carried out regularly on the used gamma camera [85-95].

Table 3.1 QC test frequency for ɣ-cameras

Test	**Frequency**
Energy spectrum display	Daily
Centering of PHA window settings	Weekly
Extrinsic or intrinsic uniformity system	Daily, weekly, half yearly
System spatial resolution	Weekly, half yearly
Extrinsic energy resolution	Daily, weekly
Sensitivity	Annually
Count rate response	Trimestrial, annually
Intrinsic spatial non linearity	Annually
Spatial distortion	Monthly
Non uniformity	Daily, weekly
Mufti-window registration	Annually
High count density collimator floods	Annual or when suspicious of damage
Whole-body accessory	Annually

Table 3.2 Operational controls test frequency for ɣ-cameras

Test	**Frequency**
Collimator and detector head mountings and collimator damage	Daily
Energy calibration of PHA	Daily
Flood field uniformity and sensitivity	Daily
Background count rate	Daily
Film handling and processing	Daily
Detector evolution	Daily
Instruction for the quantities of radioactive element to be administered	Daily
Overall check quality system	Daily
Selection and collimator qualiy system	Daily
Linearity correction and matrices validity	Daily

3.8 Tomographic Mode

These controls are not involving the rotation system. However, they are relevant for the proper function of a tomograph and condition the proper performance of quality control [96-99].

3.8.1 Mechanical Controls

- Horizontality verification of the floor, of the detection head, of the bed, and rotation axis. The gamma camera head should remain at horizontal whether is facing the floor or the ceiling.
- Verification of displayed values: position, angle, etc.
- Verification of the speed of rotation at continuous mode and angular accuracy at step by step mode.
- Security system verification.

3.8.2 Calibration of Gains in X and Y

The algorithm used for the image reconstruction is based on certain assumptions concerning the origin of the photon, hence a poor calibration of gains in X and Y can lead therefore to reconstruction artifacts.

3.8.3 Collimator Holes Angulations

There may be a difference in the orientation of holes on the collimators, which can lead to losses in the linearity resolution and uniformity defects. NEMA does not provide a test procedure to verify the parallelism of the collimator holes. However, there are some user associations such as (AAPM, IAEA) provide procedures to verify these parameters.

3.8.4 Rotating Characteristics

It is about studying the parameters which involve the rotation system but not the reconstruction software of the tomographic sections (slice).

- **Determination of Center of Rotation (COR)**

This is one of the most relevant elements of quality control in emission tomography. The detector rotates around a rotation axis, parallel line to the table of the test and perpendicular to the stative plane. To reconstruct tomographic sections, (slices) it is primordial to localize the COR, projection of rotation axis on the plane matrix image.

The COR stability during the rotation is an important parameter for cross-sections since Errors in COR of as little as 0.5 pixel in a 128 × 128 matrix can lead to degradation in image quality by its spatial resolution and contrast.

The COR also must coincide with the acquisition matrix center because the reconstruction software assumes that the projection rays augment all at the same point and that this point is located at the center of the reconstruction matrix. The constructors therefore propose a method for measuring the position of COR as well as appropriate correction algorithm. To perform this calibration the user must follow the manufacturer's instruction for data acquisition and analysis (because they correspond to the computation mode specific to the tomograph).

Naturally, it is very important to verify periodically the stability of this kind of calibration owing to mechanical problems (lack of parallelism between the plane of the detector and axis of rotation). No NEMA test is proposed. The AAPM envisages to determine and verify the COR position (this method corresponds globally to the one recommended by the manufacturers).

- **Detector Head Angular Variation**

✓ **Angular variation of the uniformity**

The uniformity of projection images is a very important factor for the quality control of tomographic images. It must remain stable during the rotation. It is therefore necessary to control its variations according to the detector orientation.

✓ **Angular variation of the sensitivity**

In similar way as uniformity, the sensitivity of the system must remain stable during the detector rotation.

✓ **Angular variation of the spectrometry**

The spectrometry stability during the rotation determines, among others, that of uniformity:

- the maximum position of total peak absorption,
- the width at mid-height of the peak as described in planar mode.

The both index must remain constant to within 1% while the camera rotates at 360°.

- ✓ **Angular image displacement and orthogonality of signals axis**

The reconstruction software of the tomographic cross-section considers that the image position of a point source does not vary during the camera rotation and the electrical axis of that are and remain orthogonal.

3.8.5 Characteristics after Reconstruction

- **Spatial resolution in the transverse plane**

The spatial resolution at reconstructed cross-sections depends on the radiation energy, presence or absence of scattering materials, reconstructions filters, size of acquisition matrix and reconstruction, the orbit used and of course the gamma camera's intrinsic spatial resolution.

- **Non uniformity of reconstructed image**

There is no NEMA standard for this very delicate parameter to determine, because the classical algorithms of non uniformity evaluation reflect poorly the ring artifacts' sometimes present on the reconstructed image, moreover they are very sensitive to the attenuation correction.

Table 3.3 Suggested test and frequency [96-99]

Test	**Frequency**
General inspection	Annually
Calibration of gains in x et y	Annually
Collimator holes angulations	Réception
Center of rotation	Weekly
Angular variation in uniformity, sensitivity and spectrometry	Annually
Angular image displacement	Annually
Spatial resolution in the transverse plane	Annually
Uniformity of reconstructed cross section	Annually
Overall performances tests	Biannual

3.9 Gamma Camera Phantoms

The use of phantoms starts from the commencement of the 20th century, using often tanks of water and blocks of wax for X-ray experiments, and to nowadays, these materials are always in employ in some applications. Subsequently, by the 1960s,

further effective tissue or material replaces and sophisticated phantoms commenced to emerge.

Nowadays, physical phantoms are utilized in carrying out large tasks in the field of diagnostic imaging and radiation therapy. This involves assessing the performance of imaging instruments, measuring radiation dosage during therapy, teaching interventional image guided methods, and maintaining equipment in the field.

Physical phantoms are the paramount devices for medical physicists to investigate about or perform medical imaging systems. These phantoms supply the means to determine, not only qualitatively but also quantitatively, the performance parameters of medical imaging systems.

As compared to computational models, test phantoms can be useful in that data are procured with a real scanner and include the impact of the parameters that effect on the entire ɣ photon detection operation. The drawback of physical phantoms, however, is the complexity of simulating the variation of the activity in an organ in time. The test phantoms thereby offer very important tools for evaluating and improving medical techniques of acquisition devices, processing and reconstructing images in vitro [101,103].

This section will provide some of the most common physical phantoms that are utilized to assess the performance parameters of ɣ-cameras. These phantoms are also known as test phantoms.

3.9.1 Why Phantoms?

To evaluate the operation status of the ɣ-camera that produces scintigraphic images, we need a reference that cannot be the patient but a phantom.

However, the choice of the phantoms is justified since it is designed to evaluate accurately certain criteria in imagery from acquisitions realized on phantoms to characterize performance limits prior to employing them for processing planning.

The phantoms are relevant tools to stimulate human anatomy and physiology and allow us to evaluate the acquisition methods and images analysis. The accurate anatomy and physiological functions of a phantom are known. The test phantoms

thereby offer very important tools for evaluating and improving medical techniques of acquisition tools, processing and reconstructing images in vitro.

3.9.2 Point Source Holders

This type of phantom is employed to maintain a point source that is used in intrinsic resolution, linearity, and uniformity assessments. It consists of lead and its principle objective is to protect the personnel, walls and ceiling and makes accurately parallel the ɣ radiation to the detector. Figure 3.8 shows a picture of a source supporter (holder) in an inclined position so as that it can point to the detectors from the floor. A copper plate has to be placed in front of the source supporter to play out as absorber and prevent the low energy photons. When put on the floor, source supporter size can be arranged such that the point source is guided to the center of the detector during the investigation [102].

Figure 3.8 Point source holder.

3.9.3 Slit Phantoms

Slit phantoms are one of the test objects employed to assess the intrinsic resolution of a ɣ-camera detector. This phantom type is made up of a thick lead mask of 0.3 cm and consisting of 0.1 cm broad parallel slits that are 3 cm spaced apart. Slit phantoms, which are normally produced by the ɣ-camera sellers, differ in size to meet perfectly to specific detectors. The mask is positioned in the nearest possible closeness to the crystal at including its complete area. Assessment is carried out utilizing a ^{99m}Tc point source centered at a distance more than five times the largest dimension of the UFOV of the crystal. The point source activity is adjusted so as that

the count rate (sensitivity) is less than 20 kcounts/s. The figure 3.9 shows a picture of the slit phantom designed for a cardiac camera which has field of view that is smaller than that of a typical ɣ-camera. Figure 3.10 shows an obtained image of the slit phantom for a typical ɣ-camera to evaluate the resolution [102].

Figure 3.9 An image of a slit phantom design.

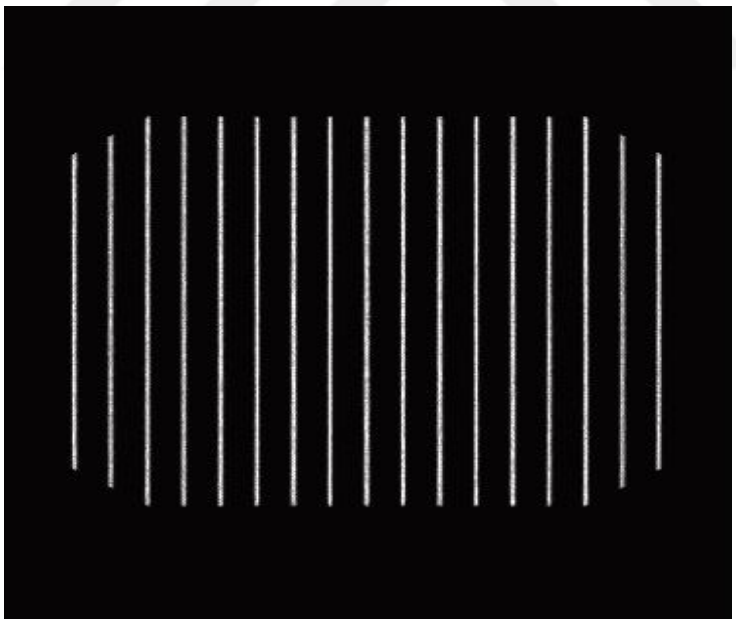

Figure 3.10 Produced image by the slit phantom to measure the resolution.

3.9.4 Bar Phantoms

The resolution test is one of the most frequent quality control tests in ɣ-camera that has to be performed through bar phantoms. These phantoms can be employed to assess, semi-quantitatively, for instance, visually, the intrinsic and extrinsic

resolution of a gamma camera. The images of phantoms can likewise be practical for the quantitative estimation of the ɣ-camera linearity which is normally assessed by slit phantoms.

These phantoms are made up of lead strips included into plastic and usually aligned in 4 quadrants. The strips are made up of different thickness for each quadrant. Figure 3.11 shows rectangular bar phantom image, which contains 4 quadrants with strip sizes of 0.2, 0.25, 0.3 and 0.35 cm (middle), whilst on the left-right part, the image has 4 quadrants with strips of sizes 0.32, 0.46, 0.63 and 0.1 cm. The two images were acquired with 512 × 512 size matrix and with a number count of ten million counts with an ADAC FORTE ɣ-camera. In the displayed images of the phantoms, there is a grey color in the maps, white lines match the plastic strips whereas black lines match the lead strips. In a bar phantom, the strips are spaced with the same space as the strip width [102].

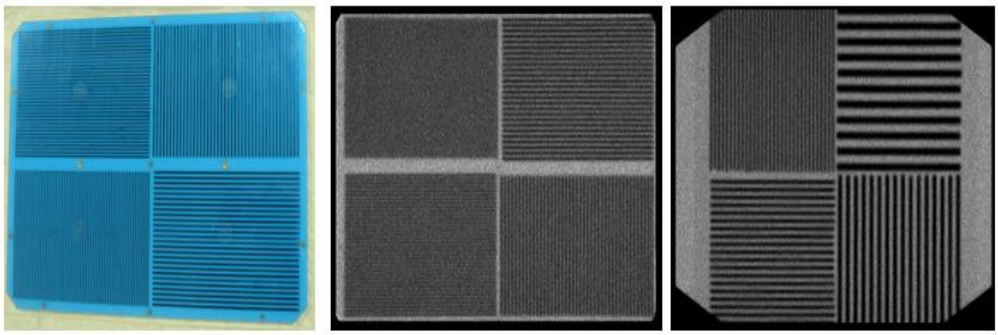

Figure 3.11 4-quadrant rectangular bar phantom.

In periodic quality control tests, usually carried out weekly or every two weeks, bar phantoms are employed for the visual measurement of the extrinsic resolution (with collimator), together with a flood source. Usually, a low energy high resolution, parallel hole collimator is employed during this test. The bar phantom is directly put on the collimator first and the flood source then is put on the top of the phantom. As the resolution of the ɣ-camera is dependent upon the distance from the detector, machinists should ensure that the bar phantom and the collimator are in direct touch between them. A ten million count image of the bars is usually obtained and estimated visually to control the detector resolution and linearity.

When employed for assessing the intrinsic resolution, the bar phantom is also put upon the detector with collimator removed, and ^{99m}Tc point source is put at a distance 5 times the largest dimension of the crystal away from the bar phantom [102].

3.9.5 Dual-line Phantom for Whole-Body Imaging

Dual-line phantom is employed to measure the whole-body resolution of a ɣ-camera system, as shown in Figure 3.12. This phantom composes of two parallel line sources. The lines are consisting of 0.1 cm in internal diameter and 10 cm center to center. Figure 3.12 presents a custom-built, dual-line phantom. The line is normally filled with ^{99m}Tc activity with a concentration of about 10 mCi/mL to obtain a satisfactory count rate. During the measurement, the line sources are positioned at a distance of 10 cm from the collimators. When evaluating the perpendicular resolution, the lines have to be adjusted parallel to the direction of the bed with one of them being in the center of the bed. When evaluating the parallel resolution, the lines must be placed perpendicular to the bed direction movement. The whole-body resolution is estimated from the FWHMs of the line profiles extracted from the image of the dual-line sources.

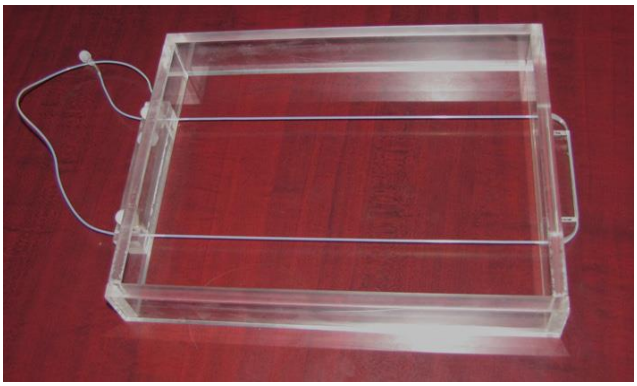

Figure 3.12 Dual-line phantom for whole body resolution tests [102].

3.9.6 Planar Sensitivity Phantoms

In planar sensitivity test, the precision of the detector response to a radioactive source of known activity is evaluated for the specific collimator. It is proposed to employ a Petri dish containing about 0.3 cm of water homogeneously mixed with an adequate activity of about 40 MBq of ^{99m}Tc. The activity has to be drawn into a syringe and then assessed properly in the dose calibrator. After the activity injection in the Petri dish, the remaining (residual) activity in the syringe has to be evaluated.

The remaining activity is removed from the initial activity to determine the net injected activity into the dish. This dish has to be put at a distance of 10 cm from the face of the collimator. It is suggested to obtain two images. The average count, in units of counts per MBq per second or count per minute per mCi, is determined to evaluate the planar sensitivity of the system [102].

3.9.7 Total Performance Test Phantoms

Image quality assesses or global SPECT system performance, including noise, tomographic uniformity, contrast, and lesion detectability which are assessed employing overall performance phantoms. These kinds of phantoms are found in the market and are difficult to make in a workshop. There are many commercial phantoms for this purpose [102].

3.9.8 Carlson Phantom

This phantom is designed and developed by Carlson. These types of phantoms are often employed for assessing the noise, tomographic uniformity, linearity, and image contrast. As shown in Figure 3.13, the phantom has a main source tank, which is made up of acrylic with dimensions: 203.2 mm inside diameter, 215.5 mm outside diameter and 304.8 mm length. It has different inserts, which are shown below in Figure 3.13.

The thick plastic screws on the top cover permit facile filling and emptying out of the tank with water. The ^{99m}Tc liquid injected inside the tank plays out as the background activity, which may be about 300 and 500 MBq, according to the collimator used.

There is a section or an insert for each performance characteristic. The SPECT uniformity is measured employing the uniform part of the phantom. The non uniformities in the ɣ-camera may result in serious ring artifacts. The artifacts can be checked for by verifying at the uniform transverse slices. The noise can be quantitatively evaluated from the uniform part.

As shown in Figure 3.13, on the left side of the picture: a crossed network of cut out channels, in an acrylic block, can be employed to measure the linearity. The region where only background activity is available is utilized to assess the SPECT uniformity. In the middle of the image: 8 pairs of holes drilled, with diameters of 4.7,

5.9, 7.3, 9.2, 11.4, 14.3, 17.9, and 22.3 mm (hot lesions). On the right side of the image: 7 rods consist of 5.9, 7.3, 9.2, 11.4, 14.3, 17.9, and 22.3 mm in diameters, simulate cold lesions [102].

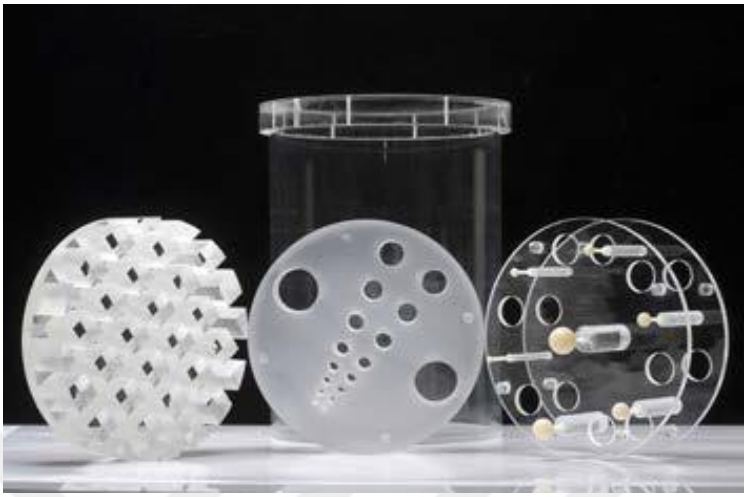

Figure 3.13 Carlson's phantom tank and its all three inserts.

3.9.9 Jaszczak Circular and Elliptical Phantoms

These phantoms are similar to the Carlson phantom, they are employed to measure the total performance of tomographic or SPECT systems following a repair or preventive maintenance, or during acceptance testing or periodic testing. Besides, these phantoms can be employed in assessing the effect of reconstruction filters on resolution, as well as for other aims in research studies.

These phantoms compose of a basic tank or cylinder made of acrylic with various inserts, as shown in Figure 3.14. These phantoms can be in circular or elliptical tanks. The cylinders of all models of the circular flanged phantoms possess same physical particularities: 216 mm inside diameter, 186 mm inside height and 32 mm wall thickness. The main dissimilarities between the various models of the flanged cylindrical phantoms are the rods diameters and the solid sphere inserts. The circular phantom has two varieties: flanged and flangeless. These varieties are developed to measure a range of systems, from low to ultra-high resolution, which has spheres and rods smaller than the others.

All the phantoms of Jaszczak are made up of six sets of cold rods and six solid spheres. In flanged varieties, the sizes of the spheres differ. In each set, the number of the rods relies on the rod size in that set as various models of the phantom have

rods of various sizes. In flangeless varieties, the spheres diameters are 0.95, 0.127, 0.159, 0.191, 0.254 and 0.318 cm, whilst the diameters of the rod are 0.48, 0.64, 0.79, 0.95, 0.111 and 0.127 cm. The solid spheres and rod inserts both imitate cold lesions in a hot background. Spheres are employed to assess the image contrast whilst the rods are employed to evaluate the image resolution in tomographic systems [102].

Figure 3.14 Jaszczak phantom employed for checking image quality.

3.9.10 Hoffman Brain Phantom

This phantom was designed and developed by Hoffman, as shown in Figure 3.15, which is used to provide anatomically proper simulation of the radioactivity distribution in typical brain. Utilizing this phantom, metabolic activity and cerebral blood flow in the brain can be simulated. It can be employed in both SPECT systems and PET to optimize and evaluate imaging acquisition protocols, to measure scatter and attenuation correction methods, and to assess the performance of imaging systems. It is made up of a water fillable cylinder comprising 19 separate layers each 0.64 cm thick. The water volume is about 1.2 liter. Water can freely penetrate between layers to simulate concentration ratios of 4:1:0 between white, grey and ventricle, respectively, in normal brain [102].

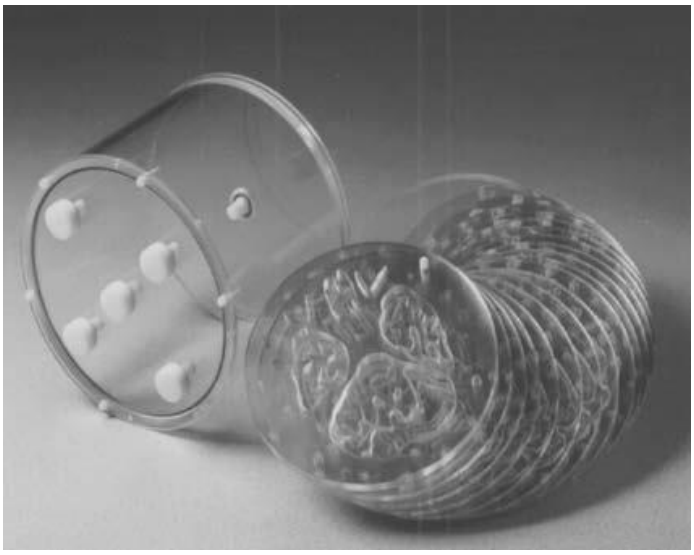

Figure 3.15 Hoffman phantom with a water fillable cylinder and layers of inserts.

CHAPTER IV

MATERIAL AND METHODS

This chapter will provide the methodology and realization techniques of the in-house phantom. Also, the technique of experimental setup, as well as the methods and materials which are employed in the thesis will be presented in this chapter.

4.1 Phantom Preparation and Experimental Methods

4.2 Test Objects or Phantoms

In nuclear medicine, as in other fields, it is necessary to use test objects or phantoms which permit to adjust, calibrate, or to quantify the performance characteristics of the imaging equipment. We use hence phantoms which are very different in their designs. In nuclear medicine by which an emission image is made, usually, phantoms used are made up of sealed containers which can be filled with a radioactive liquid solution of varying concentration. [102,103].

4.3 Phantom's Characteristics

Due to the detector physical characteristics (resolution, sensitivity, linearity, etc) and interactions between radiation and matter (attenuation and Compton scattering) obtained image through the gamma camera imaging system using a phantom, should provide a less or more accurate representation of the studied quantities or dimensions (radioactive concentration, size objects, contrasts, etc). It is therefore necessary to use test objects or phantoms whose physical characteristics are (in the ideal case) perfectly known in order to establish a relationship between the image obtained and the object used.

4.4 Variability of Activity

In planar scintigraphy examination, we essentially take into account the variability of the activity of a region of interest or in the activity of this same region. This is also permitting to determine the performance characteristics of the ɣ-camera.

Phantoms are traditionally made from plexiglass materials, a brand of acrylic PMMA (polymethylmethacrylate) material, which has many benefits and is available in a wide spectrum of colors and opacities. It can be molded into a variety of shapes including tubes, cylinders, large sheets, etc. and can also be machine manipulated and drilled. It is one of the most common and preferred materials for phantoms due to a few specific characteristics: highly transparent, highly impact-resistant, easy to clean and polish, highly durable, light, easy to transport, highly scratch and shatter-resistant. Furthermore, its density (1.17 to 1.20 g/cm^3) is similar to human being tissues and, as such, this material is bio-compatible. All of these characteristics make it an ideal material to serve as a quality control tool to measure gamma camera performance [104-106].

In order to respond to the requirements or recommendations set by international organizations for quality control, a cylindrical phantom has been designed. It should be stressed that the acquisition of ideas and design of the phantom were based on the recommendations of the National Electrical Manufacturers Association NEMA (NEMA 2001).

4.5 Proposed Phantom

The phantom was fabricated in-house. As seen in Figure 4.1, it has a cylindrical shape with a diameter of 230 mm and thickness of 60 mm divided into two large sections (left and right). The right part consists of five series of cylindrical holes (A, B, C, D, and E). The diameters were different for each line of holes, 25 mm, 20 mm, 15 mm, 13 mm, 8 mm, 6 mm, and 4 mm, and these were drilled to different depths, 15 mm (A), 12 mm (B), 10 mm (C), 8 mm (D), and 7 mm (D), with a 4-mm distance between holes and an angular spacing between the sets of holes of 45°. The left part was divided into two series of slits (F and G), each 5 mm in diameter with exactly the same 6-mm depth but different lengths; the widths and the spaces between these were exactly 4 mm, with the slits drilled in two perpendicular parts (F and G). Figure 4.2 shows a photograph of the phantom, a pattern of its main form, and the cover (240 mm diameter and 10 mm thick). Figure 4.3 shows the in-house phantom during its fabrication process.

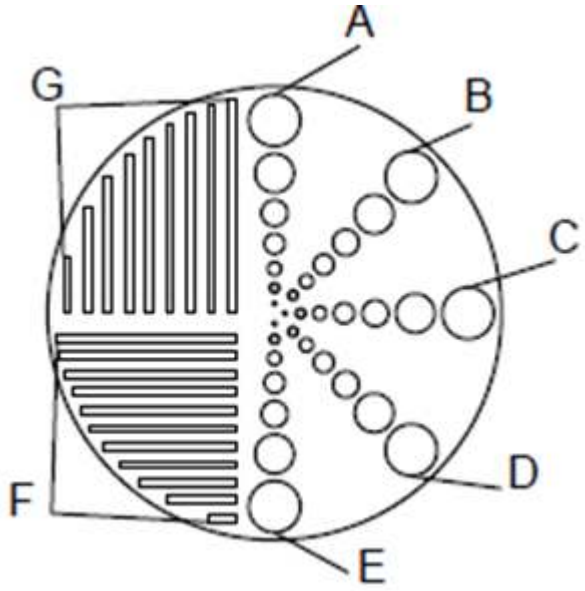

Figure 4.1 A schematic of the phantom's shape [107].

Figure 4.2 A photograph of the realized phantom and its cover [107].

Figure 4.3 A photograph of the in-house phantom under the fabrication process.

4.6 Gamma Camera and Image Acquisition

This study was carried out in the Nuclear Medicine Unit of Gaziantep University Hospital using a double head detector SPECT gamma camera, model Forte With Jetstream, manufactured by Philips (model No. B04080073), as shown in Figure 4.4 [108, 109]. It was fitted with a low energy high resolution (LEHR) collimator, the thickness of the NaI(TI) crystal: 9.5 mm, size of the crystal: 508 × 381 mm, number of the photomultiplier tube: 49. The SPECT system was verified to ensure that the photo-peak was centered at the 140 KeV gamma line window of the radiotracer ^{99m}Tc widely used in diagnostic and detector had an energy solution of 15% at 140 KeV, as shown in Figure 4.5. Figure 4.6 shows a photograph of the phantom at the workstation computer used for the acquisition of the images during the experimental work.

Figure 4.4 A photograph of the tested gamma imaging system.

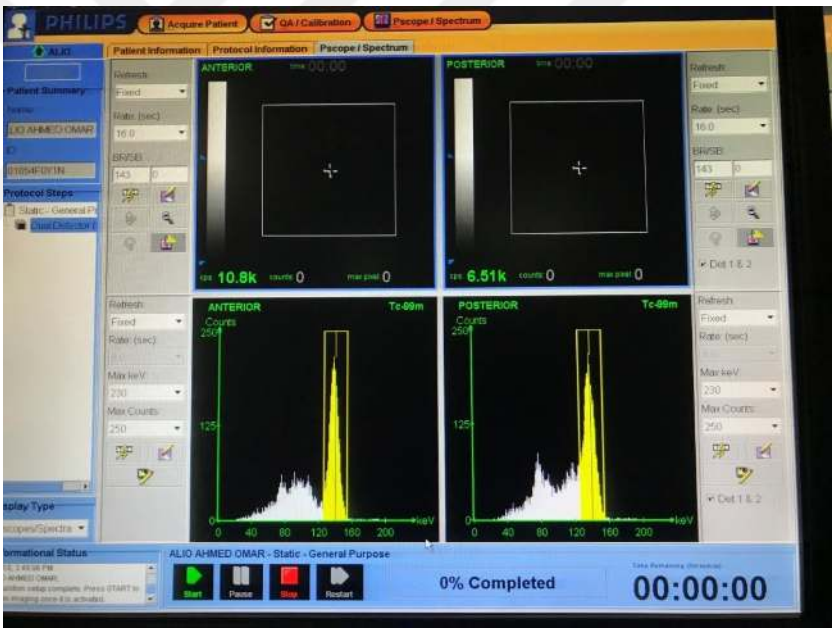

Figure 4.5 Photo-peak window of ^{99m}Tc centered at 140 KeV.

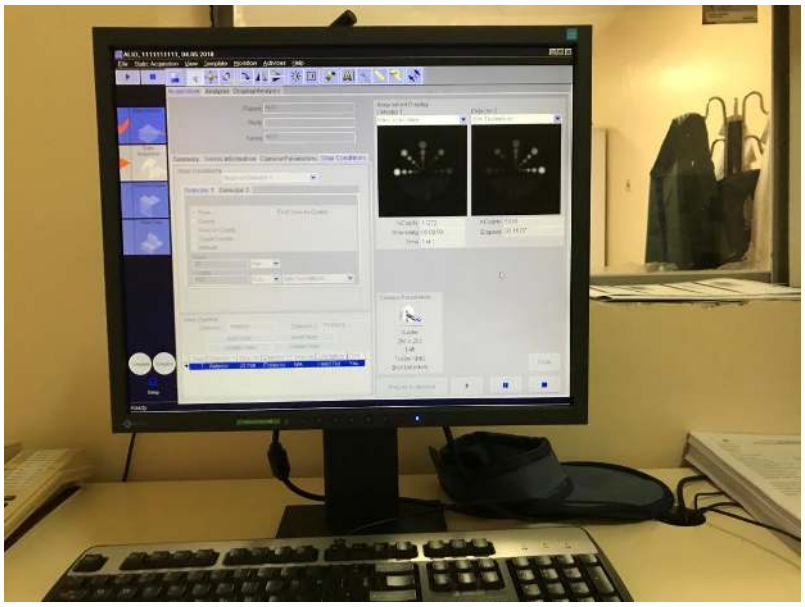

Figure 4.6 A photograph of the phantom at the workstation computer.

4.7 Experimental Methods

Initially, a radioactive solution to fill the phantom was prepared. A sample of ^{99m}Tc was collected from the hospital's generator on a daily basis. This was dissolved in a solution of sodium chloride (0.9%: physiological saline) and had an activity of 7.4 × 10^{-1} GBq/ml, which was diluted with distilled water to 1.85 × 10^{-1} GBq/ml ^{99m}Tc. The phantom was filled with radioactive material using a syringe, to control for air bubbles and ensure the homogeneity of the radiotracer. The acquisition was carried out with one head while the phantom was in the patient's bed under the detector. The phantom was placed under the head to cover the region of interest in the field of view. The image was acquired with a 256 × 256 × 16 matrix size and the photo-peak centered for ^{99m}Tc at 140 KeV with a 15% window, using a count mode of 250 million counts over 1200 seconds at a rate of 160 counts per second - static type. CFOV (Central Field of View) calculations were carried out to consider approximately 75% of the diameter of the detector. For each experiment, a sum of 10 million counts was used to assess integral uniformity. The same procedure was performed at various distances (5, 10, and 15 cm) between the phantom to the detector and at different times (i.e., three experiments conducted at two-month intervals). Uniformity was effectively assessed in the central 75% area of the homogeneous image. The uncertainties associated with the measurements were approximately 1.9%. The mean pixel values in the region of interest were calculated. Likewise, (IU and DU values) for the CFOV (Central Field of View) and UFOV

(Useful Field of View) were calculated according to the method originally provided by the NEMA for quality assurance of nuclear medicine gamma cameras. The NEMA method uses maximum and minimum counts per pixel within the region of interest and average counts over nine neighborhood pixels. Subsequently, the count values measured in the nine adjacent pixels were considered to be the maximum and minimum counts observed in the CFOV [110, 111]. Lastly, the assessment of IU (integral uniformity) and DU (differential uniformity) indices for the UFOV and CFOV of the gamma camera can be calculated according to the NEMA, IAEA, and AAPM (American Association of Physicists in Medicine) guidelines, as expressed in Equations (3. 1) and (3. 2).

Prior to put the phantom on its measurement position, the atmospheric and electrical conditions have been verified. Thus, the measurements were carried out at a 20°C of temperature under normal atmospheric pressure (about 1002 hPa), with a humidity of 50 %. The machine voltage supply via an inverter was (220 ± 5) V.

Table 4.1 Activities contain in the each compartment of the phantom

Activities in mCi						
Holes					**Slits**	
A	**B**	**C**	**D**	**E**	**F**	**G**
8.45	6.75	5.65	4.5	3.95	0.27	0.23
4.75	3.8	3.15	2.5	2.2	0.27	0.15
2.45	1.95	1.65	1.3	1.15	0.17	0.10
1.45	1.15	0.95	0.75	0.65	0.12	0.10
0.9	0.75	0.6	0.5	0.43	0.11	0.10
0.7	0.55	0.48	0.38	0.33	0.10	0.12
0.055	0.045	0.035	0.03	0.025	0.09	0.11
-	-	-	-	-	0.08	0.07
-	-	-	-	-	0.05	0.042
-	-	-	-	-	-	0.041
-	-	-	-	-	-	0.025

4.7.1 Experiment One

The phantom was placed in a horizontal position 5 cm from the detector and exposed for 15 minutes; the resulting image is presented in Figure 4.7. The upper left quarter of Figure 4.7 contains inhomogeneities that likely resulted from improper technique when filling the phantom with the radioactive solution. In the lower left quarter, this

type of inhomogeneity is absent because proper technique filling was realized when filling the phantom. On the right-hand side of Figure 4.7, higher intensities were observed, which was expected since the activity contained within the holes is theoretically more important due to their volume, as can be seen in Table 4.1.

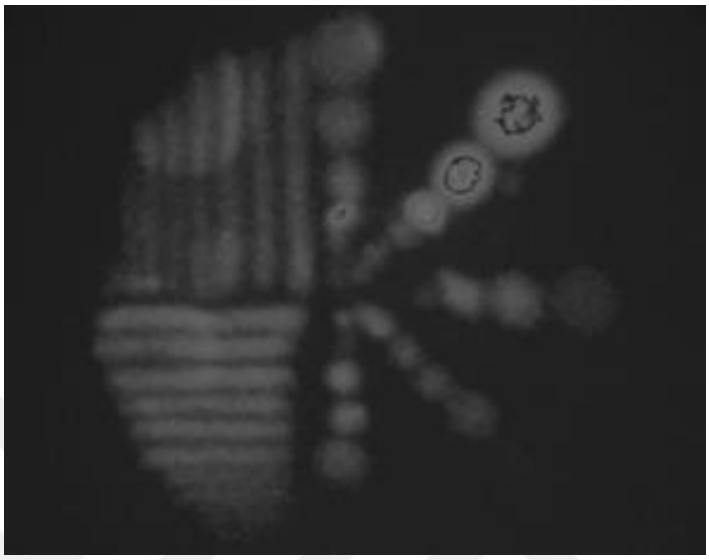

Figure 4.7 Gamma image shows the phantom at 5 cm imaging distance [107].

From experiment one, a number of conclusions can be drawn:

- The radioactive solution must be mixed well, and the phantom must be filled up carefully in order to avoid any radiotracer inhomogeneities.
- The phantom should be placed a good distance (at least 10 cm) away from the detector in order to avoid overlapping activities in the different holes and slits.
- The phantom should be placed horizontally and behind the camera head, in the extreme case of the entire phantom being moved 0.5 mm away at 5 cm, one would expect a change due to an r^2 of ~2%, which will affect the measurement.

4.7.2 Experiment Two

Given the findings from the first experiment, the phantom was emptied, cleaned, and not used for two months. At this point, it was filled with a well-mixed solution (agitated by vortex) of ^{99m}Tc 1.295×10^{-2} GBq that was bubble-free and maintained ^{99m}Tc homogeneity. The phantom was placed about 10 cm from the detector, and the run time was set to 15 minutes. The obtained image can be seen in Figure 4.8 and has some discontinuities on the sides of the slits. These discontinuities are likely due to the effect of the surface tension on the walls, which indicates that filling the slits was

poorly executed. Hence, this phenomenon was not observed at the hole level, especially those with large diameters. A slight radiological blur was also observed in this image, which could potentially be removed by placing the phantom away from the detector. As a result, the quality of the image improved relative to previous ones.

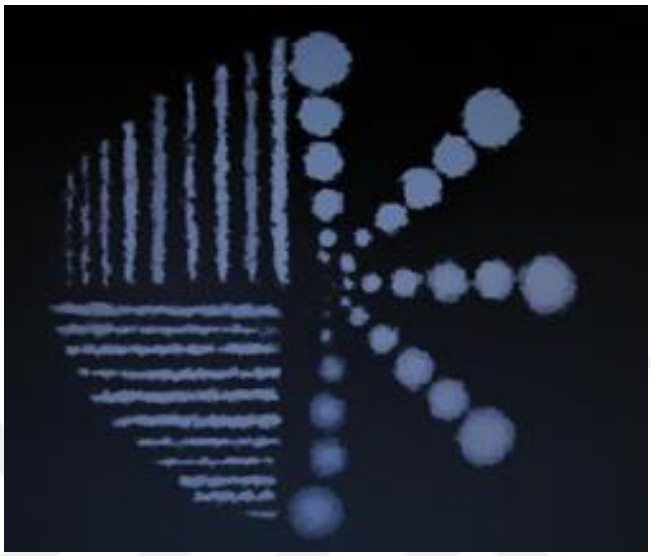

Figure 4.8 Gamma image shows the phantom at 10 cm imaging distance [107].

4.7.3 Experiment Three

In this last experiment, a more homogeneous filling was performed, conforming to the same steps and conditions mentioned above were performed for filling up the phantom with ^{99m}Tc 1.295 × 10^{-2} GBq. The phantom was placed to the detector at a distance of 15 cm. The results are presented in Figure 4.9, where images were evaluated in terms of uniformity, linearity, contrast, spatial resolution, and sharpness.

Figure 4.9 Gamma image shows the phantom at 15 cm imaging distance [107].

4.7.4 Intrinsic Uniformity

In order to demonstrate the utility of this technique, another comparison of intrinsic uniformity test was performed. As seen in Figure 4.10, intrinsic uniformity measurements were made using a point source of ^{99m}Tc to compare to those made by the in-house phantom. We initially followed the manufacturer's instructions for the quality control test. Collimators were removed from the head. A point source of ^{99m}Tc with an activity of 1.295×10^{-2} GBq was placed where the distance from the point source to the detector was at least four times the CFOV diameter. The image matrix size was 256 × 256, its energy window was adjusted to within 15%, and the count rate was 15 kcps (Kilo count per second). The gamma camera was equipped with software with which both the integral and differential values were automatically calculated using the formulas (3. 1)-(3. 2) [92, 94]; these results are presented in Table 5.1.

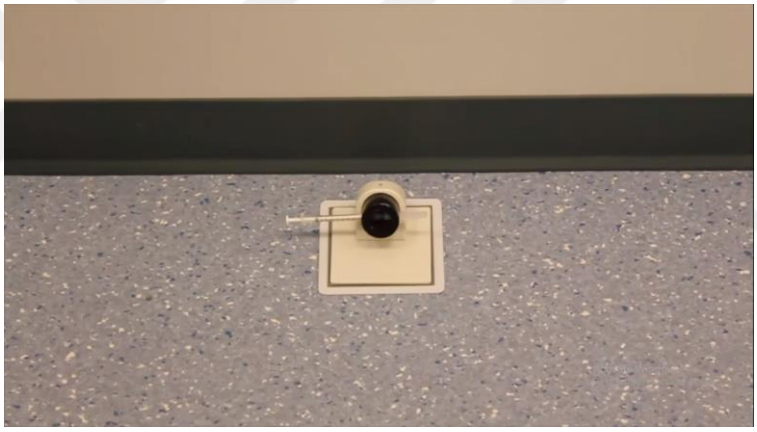

Figure 4.10 A photograph of the point source used for the uniformity test.

CHAPTER V

RESULTS AND DISCUSSIONS

In this chapter, the results obtained using a developed in-house phantom to check the performance characteristics of a gamma camera, and the discussions are provided.

5.1 Results

The outcomes described here provide an example of an affordable and technically useful phantom device and its application to extrinsic uniformity, spatial resolution, linearity, and contrast measurements in the routine quality control of a gamma camera using ^{99m}Tc.

The results presented in Figure 4.9 were used to assess the measured activity profile by scanning the series of wells (A). This profile was obtained using one of the applications installed in the gamma camera (Menu - Quality Assurance - Uniformity). For each hole, the corresponding measured activity was extracted from the imaging data and recorded. Next, the real activities were plotted on the x-axis and measured activities on the y-axis in GBq and compared; a high level of correlation was observed between the two data series, as shown in Figure 5.1. Thereby, using the least-squares method, a linear regression of these points was generated. There was indeed a significant positive association between the measured activity and the corresponding real activity with a slope of $0.8308x + 0.0045$, correlation coefficient $r = 0.99$, and $p < 0.01$, which is consistent with a linear correlation with a high confidence level. Therefore, the resulting line was straight and well fit to the data. The errors bars represent standard error estimates [107].

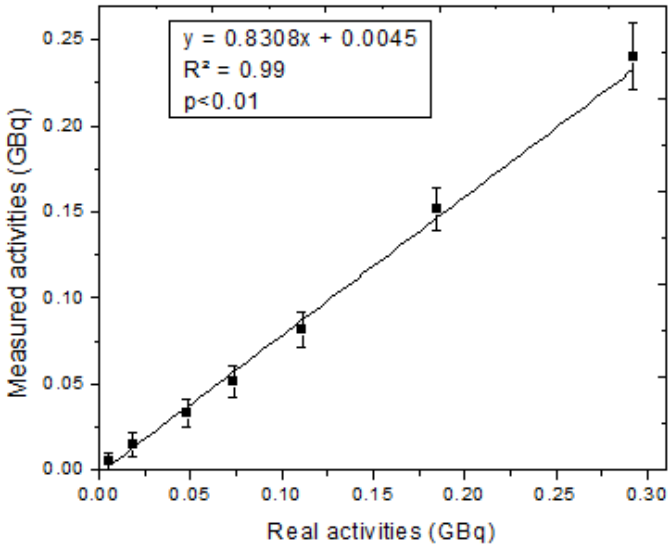

Figure 5.1 The relationship between the measured and real activities of the holes (A).

Figures 5.2 and 5.3 showing optimum values of the integral and differential uniformity at UFOV and CFOV have been obtained from different distances of 5, 10, and 15 cm (in-house phantom source-detector), respectively. The integral uniformity for CFOV was between 1.93% and 2.30% whilst the integral uniformity for UFOV was between 1.90% and 2.40%. The differential uniformity for CFOV was obtained between 1.48% and 1.60% whilst the differential uniformity for UFOV was between 1.55% and 1.70%. The integral uniformity range was found to be between 1.93% and 2.40% and differential uniformity has a range between 1.48% and 1.70%. In Figures 5.2 and 5.3, both the IU and DU uniformity of UFOV and CFOV improved when phantom-to-camera distance augmented. The error bars in Figures 5.2 and 5.3 represent the standard error. The results shown in Table 5.1 give the IU and DU values for UFOV and CFOV using a point source of ^{99m}Tc. Calculated uniformity indices for the images acquired above by the in-house phantom were compared with uniformity indices obtained from the point source of ^{99m}Tc, the corresponding constructor specification, and the NEMA, as can be seen in Table 5.2. If the uniformity distortion is less than 3%, the quality is considered good and the corrections are activated. Alternatively, if the uniformity distortion is between 3% and 8%, it is necessary to calibrate the detector. If the uniformity distortion is greater than 8%, the calibration should be carried out by maintenance service. Moreover, for all measurements collected by the in-house phantom, the mean pixel values in the region of interest were recorded, with the mean integral uniformity values falling

between 13 and 14.3%, which were within the acceptable range. Ten million counts were acquired for each image and these images had identical levels of associated uncertainty (1.9%).

Comparing the results obtained using the in-house phantom with the results of the point source of ^{99m}Tc indicated that the gamma camera's uniformity was within an acceptable range. Thus, by evaluating the images acquired throughout this experimental work, it became clear that the quality of the scintigraphy images depends not only on the radioactive source, acquisition time, and sensitivity of the collimator but also on the variation in the distance between the phantoms and the detector head.

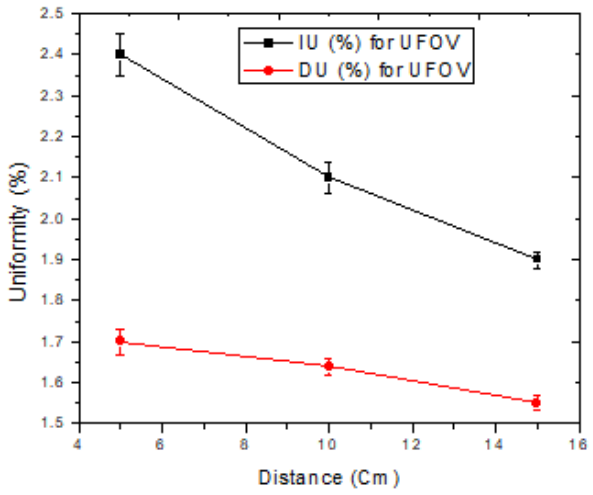

Figure 5.2 IU and DU relative to phantom-to-camera distance for UFOV [107].

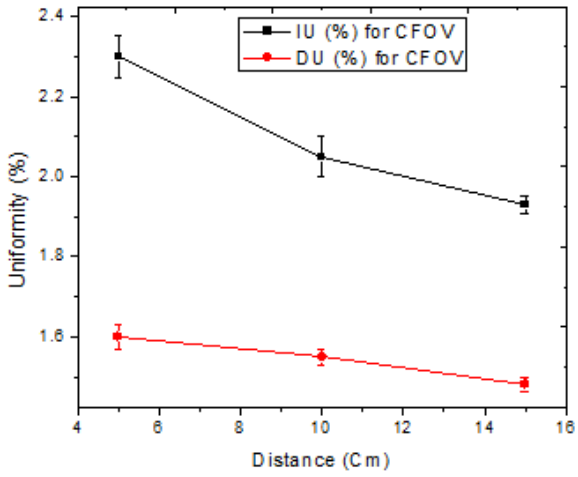

Figure 5.3 IU and DU relative to phantom-to-camera distance for CFOV [107].

Table 5.1 presents the integral and differential uniformity of UFOV and CFOV obtained using a point source filled with ^{99m}Tc were compared with uniformity indices obtained from the corresponding constructor specification. Table 5.2 shows the integral and differential uniformity indices of UFOV and CFOV allowed by the National Electrical Manufacturer Association (NEMA) [107].

Table 5.1 Uniformity, mean, SD, and constructor specification of the detector

Uniformity		**Detector**	**Constructor specification**
UFOV	Integral Uniformity (%)	2.05	<3.74
	Differential Uniformity (%)	1.33	<2.74
CFOV	Integral Uniformity (%)	1.81	<2.94
	Differential Uniformity (%)	1.38	<2.54
Mean (±SD)	-	1.6 (±0.34)	<2.99 ((±0.52)

Table 5.2 IU and DU values of UFOV and CFOV were proposed by the NEMA

Field of view	**Integral uniformity (%)**	**Differential uniformity (%)**
UFOV	≤8	≤5
CFOV	≤5	≤4

5.2 Discussion

The different depths and diameters of the holes lead to differential amounts of radioactivity contained in the volume of each hole, as can be see Table 4.1. Thus, from the images collected from these holes, the intensity differences within holes were considerably more distinguishable than between the slits. This facilitates the study of closely related contrast and spatial resolution: variations between holes enable the examination of the spatial resolution, integral uniformity, and differential uniformity, and contrast of the detector. Moreover, the gamma camera reproduced, with a high degree of uniformity, images of the slits of the phantom with the radioactive solution. This is permitted us to analyze the uniformity, linearity, spatial resolution, and contrast of the images and energy resolution of the gamma camera. Indeed, the machine is equipped with applications, from which and through the reproduced images by the phantom allows checking these performances. However, in this study, the spatial resolution and other parameter values were evaluated visually,

because the detector could distinguish small details at 4 mm distance between the slits so even the smallest holes could be faithfully observed, as seen in Figure 4.9. This study focused on the determination of the uniformity aspect, as it is the most frequently utilized performance feature in the daily quality maintenance of gamma cameras. The results of the integral uniformity and differential uniformity analyses obtained using the in-house phantom and point source of ^{99m}Tc compared favorably with manufacturer and NEMA guidelines, which can be seen in Figures 5.2 and 5.3 and Tables 5.1 and 5.2. Therefore, the level of uniformity was within the recommended range and all measurement averages were within the acceptable limits. From our data, it is clear that by increasing the source-to-detector distance either intrinsic or extrinsic uniformity improved, as can be seen in Figures 5.2 and 5.3.

Despite the technical constraints encountered during the application of the in-house phantom and experimental work, our findings support that this phantom is, with some improvements, in accordance with the different calibration protocols for a gamma camera and can be easily incorporated into quality control procedures. This phantom is intended as a comprehensive quality control tool that is a simple and affordable solution for daily quality control when alternative phantoms are not available. In order to carry out the experiment, radioactivity levels between 1.85×10^{-2} GBq and 2.96×10^{-2} GBq should be used, similar to a radionuclide in clinical studies.

Moreover, using this tool, any nuclear medicine department can build or reformulate their own in-house protocol to assess the daily variation of uniformity, resolution, linearity, contrast, and energy resolution parameters, which are suitable and acceptable. Although this phantom is well-suited; it was not intended to check each gamma camera performance. Rather, the objectives were to determine its unique capabilities and potential limitations in future studies. However, the phantom exhibited some differences from those that are designed or recommended by the manufacturer, NEMA, and user due to its geometrical form, however, the combination of holes and slits is, in fact, an advantage. Therefore, this system can evaluate the performance of a gamma camera in terms of uniformity, spatial resolution, energy, linearity, and contrast; even though these parameters are not all investigated during the experimental work, apart from the uniformity parameter.

Future studies should include analyses of additional aspects of imaging such as spatial resolution, energy, linearity, and contrast.

5.3 Comparison of Realized Phantom with Other Techniques

We present here another type of phantom technique made of plexiglass material with a geometrical shape which is different from our phantom, as can be seen in Figures 5.4 and 5.6 with their respective produced images in Figures 5.5 and 5.7. These phantoms are employed to determine the performance characteristics of a gamma camera, including uniformity, energy resolution, spatial resolution, and contrast.

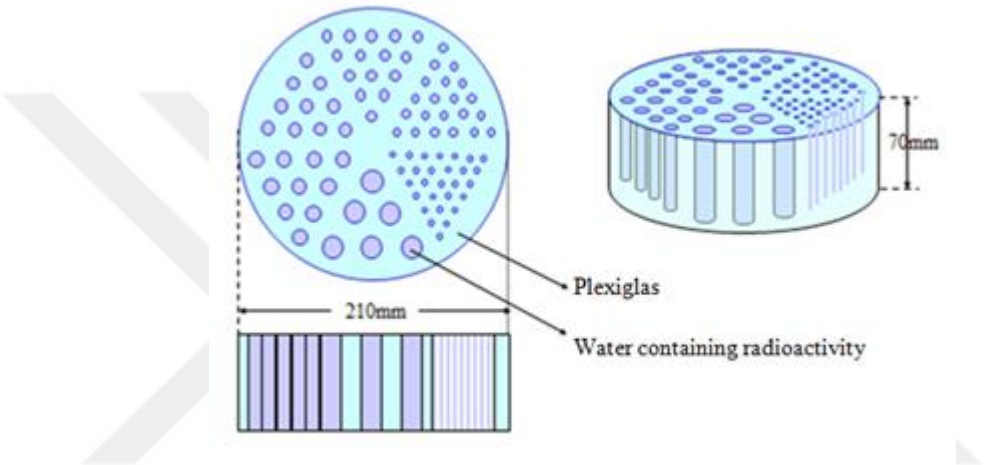

Figure 5.4 Diagram of phantom made of plexiglass with 210 mm and 70 thick. The distance between holes equal hole diameter (in mm) [112].

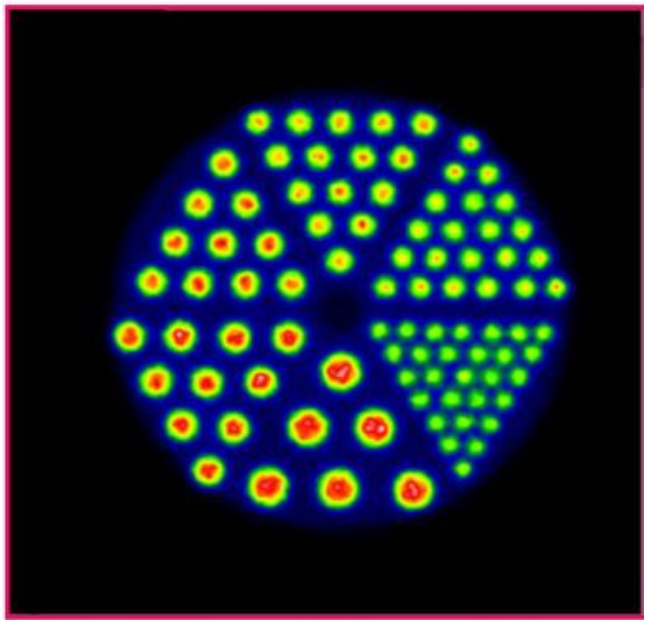

Figure 5.5 Image of a plexiglass phantom [112].

Figure 5.6 shows Jaszczak Phantom. It consisted of plexiglass with a 200 mm in circumference. This cylindrical phantom includes multiple portions of assessment of a ɣ-camera SPECT data. On the right part of the schema which contains a volume of liquid that is utilized to test uniformity. In the center part of the phantom, the rods are consisted of various diameters to determine resolution. On the left part of the phantom, there are cold spheres for supplemental resolution assessment. In certain phantoms, these cold areas or spheres are hollow which permits the user to add more quantity of activity on the surrounding media, which having hot spheres at various sizes [102].

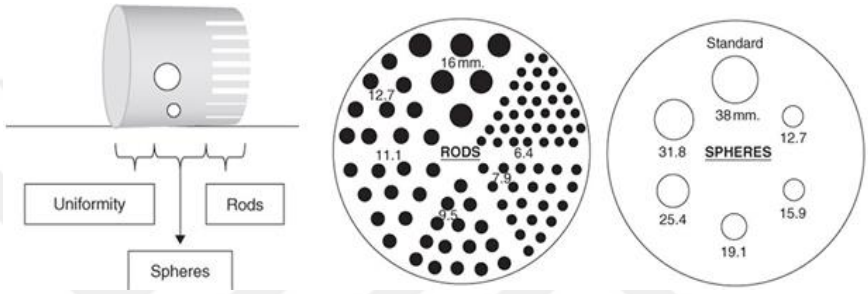

Figure 5.6 Diagram of Jaszczak Phantom [102].

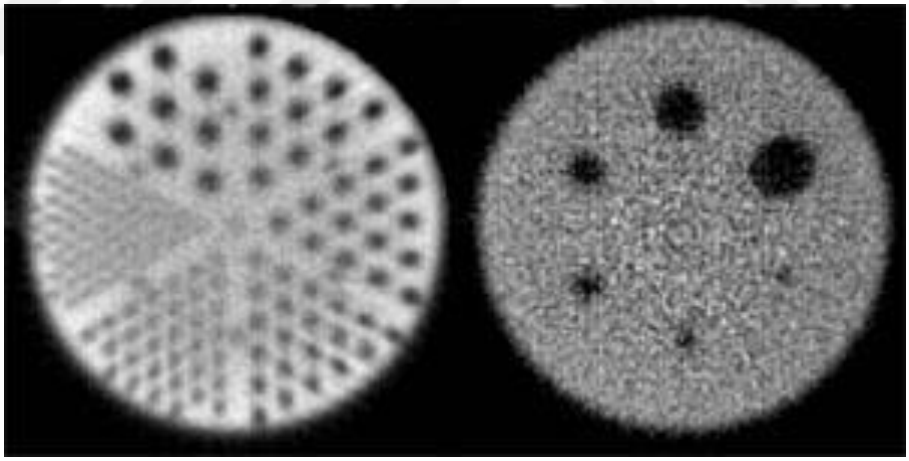

Figure 5.7 Acquired image by Jaszczak Phantom [102].

By comparing the in-house phantom with other phantoms, we can see that it has advantages. Firstly, it is cheap compared to commercial phantoms because it is realized with local materials and techniques. On the other hand, technically it has the advantage of being made up of two different geometrical forms which are slits and holes. This particularity allows studying simultaneously resolution of two different geometrical forms. Furthermore, the fact that each hole has a different volume, this is allowing to study the detector response at different activities levels. The position of

the different series of the holes (0, 45, 90, 135, and 180°) that permits to study the performance under different irradiation conditions. Finally, it is apparent that the in-house phantom offers more possibilities of study than the phantom that made of a single geometrical form. However, the in-house phantom presents the inconvenience of being difficult to fill. Indeed, the patterns of the phantom must intercommunicate with each other, in order that the filling would be done quickly and uniformly.

CHAPTER VI

CONCLUSION

Nuclear medicine is characterized by its system evolution over its history course, which has been recently further accelerated, due to its technological developments, software, and particularly radiopharmaceutical components.
The effectiveness of a scintillation camera quality control procedure is based on the system's environment and its clinical use. The use of phantoms in nuclear medicine enables optimizing clinical protocols as well as validating correction methods and protecting patients against the consequences of false clinical examination results.

The implementation of a quality control phantom is an important aspect in a nuclear medicine department. In order to ensure good quality scintigraphic images, it is necessary to execute the protocols of maintenance on a regular basis and to ensure the correct calibration of the ɣ-camera.

In this context, we have started by reporting the generalities on the basics of nuclear medicine elements. Then, we have presented the principle technique of scintigraphy, the physical bases of detections of ɣ photons, and the different components of the ɣ-camera detector.

Firstly, we were able to demonstrate how much it is important to implement proper tools, such as phantoms for performing the QC of a ɣ-camera in the nuclear medicine department.

It has been also described in the literature that the main points of how to handle a ɣ-camera starting from its installation time to its whole operation life include the followings: the acceptance testing, periodic testing which prove that everything has to match to the manufacturer's specifications, and preventive and corrective maintenances on a ɣ-camera during its use to prevent any malfunctioning have to be

fulfilled. By following the protocols established by the international organizations and users, for instance, NEMA, IEC, AAPM, and IAEA, etc. Owing to this the design and development of phantom has been chosen which is a necessary tool to be employed to overcome certain difficulties imposed or caused by lack of technology or availability of means in certain nuclear medicine department, particularly in developing countries in order to be able to test the performance characteristics of a ɣ-camera.

The design and implementation of a phantom permit us through the acquired images to characterize the ɣ-camera performance characteristics and thus to ensure the safety of the measurements. Indeed, performing parameter measurements allows us to minimize patient exposure to radiation, false patient diagnostic analysis, saving time, and ensuring its safety. Finally, we will be able to get good examination images.

Secondly, we were able to develop a phantom which was made from cylindrical plexiglass with different geometrical forms. The phantom design was based on protocols defined by NEMA and other users; AAPM, IAEA, and only used materials that are locally available and generally accessible to most nuclear medicine departments and require minimal engineering instruction. Lastly, we were able to compare the images acquired by the in-house phantom to other images obtained by standard phantoms.

The developed in-house phantom represents a simple and affordable way to test a gamma camera's performance. This may be applied, with acceptable accuracy, to the nuclear medicine field as quality control tests of a ɣ-camera. The level of the uniformity was within the acceptable range and all measurements were within acceptable averages. Furthermore, this work demonstrates that using local and affordable materials that align with NEMA recommendations, in-house phantoms can execute daily performance tests of a ɣ-camera. Particularly in developing countries, scientific support is not always readily available. Therefore, we developed a novel technique to assess and check the performance characteristic of a gamma camera, such as uniformity, linearity, resolution, and contrast. The results indicated that this method was effective and offered a good uniformity when compared with the results obtained from the point source of ^{99m}Tc. Furthermore, comparing the images acquired by the in-house phantom to other images obtained by different

techniques, one has to confirm that this device is a novel technique that can be used to check some of the gamma camera performance characteristics.

Albeit the evaluation is often complex and difficult to handle, we have tried to assess the results obtained by employing objective and subjective criteria. A maintenance engineer, the person who is in charge of the following up of the gamma camera at the Hospital of Gaziantep University evaluated the results. He confirmed that it would be greater importance to add a filling mask and tank on the prototype of the phantom that we will have more possibility of use and can be employed to test the performance characteristics of a PET.

Given the potential of this tool, the prospective studies will include optimizing the spatial resolution, linearity, contrast, and energy resolution of a gamma camera in greater detail and at higher levels of accuracy.

However, it is also important to point out that the realized phantom presents imperfections due to limited technology during its machining. Therefore, it is necessary to machine a lead filling mask so as to make easier the filling process. Furthermore, to improve the quality of scintigraphic image tests and to obtain a proper calibration of the detector response, the use of measurement masks is suggested.

REFERENCES

[1] Fahey, F., Goodkind, A., Treves, S., Grant, F., 2016. Nuclear Medicine and Radiation Protection. *Journal of Radiology Nursing*. **35(1)**, 5-11.

[2] Salditt, T., Aspelmeier, T., Aeffner, S. (2017). *Biomedical Imaging: Principles of Radiography, Tomography and Medical Physics*. Walter de Gruyter GmbH & Co KG.

[3] Arevalo-Perez, J., Paris, M., Graham, M., Osborne, J. (2016). A Perspective of the Future of Nuclear Medicine Training and Certification. *Seminars In Nuclear Medicine*. ***46*(1)**, 88-96.

[4] Saha, G. B. (2012). *Physics and Radiobiology of Nuclear Medicine*. Springer Science & Business Media. Springer-Verlag: New York.

[5] Cherry, S. R., Sorenson, J. A., Phelps, M. E. (2012). *Physics in Nuclear Medicine e-Book*. Elsevier Health Sciences.

[6] Radtke J. (2012). Nuclear Medicine Technology: Procedures and Quick Reference. *Journal of Nuclear Medecine and Technology*. **40(3)**, 207-207.

[7] Vaiano, A. (2019). Standard Operating Procedures for Quality Control of Instrumentation for Radioguided Surgery. *In Nuclear Medicine Textbook* (1079-1084). Springer, Cham.

[8] Zolle, I. (2007). Technetium-99m pharmaceuticals (1, 1). Springer: Berlin, Heidelberg.

[9] Anger H. (1958). Scintillation Camera. *Review of Scientific Instruments***.** **29(1)**, 27- 33.

[10] Zanzonico, P. (2008). Routine Quality Control of Clinical Nuclear Medicine Instrumentation: A Brief Review. *Journal Of Nuclear Medicine*. **49(7)**, 1114-1131.

[11] Graham, L., Fahey, F., Madsen, M., van Aswegen, A., Yester, M. (1995). Quantitation of SPECT Performance: Report of Task Group 4, Nuclear Medicine Committee. *Medical Physics*. **22(4)**, 401-409.

[12] O'Connor, M., Vermeersch, C. (1991). Critical Examination of the Uniformity Requirements for Single-photon Emission Computed Tomography. *Medical Physics*. **18(2)**, 190-197.

[13] DeWerd, L. A. (2014). *The phantoms of medical and health physics*. M. Kissick (Ed.). Berlin: Springer.

[14] Hines, H., Kayayan, R., Colsher, J., Hashimoto, D., Schubert, R., Fernando, J., Simcic, V., Vernon, P., Sinclair, R. L. (1999). Recommendations for Implementing SPECT Instrumentation Quality Control, *European Journal of Nuclear Medicine and Molecular Imaging*. **26(25)**, 527-532.

[15] Zimmerman, B. E., Grošev, D., Buvat, I., Pérez, M. A. C., Frey, E. C., Green, A., Quadir, K. A. (2017). Multi-Centre Evaluation of Accuracy and Reproducibility of Planar and SPECT Image Quantification: an IAEA phantom study. *Zeitschrift für Medizinische Physik*. **27(2)**, 98-112.

[16] Murphy, P. H. (1987). Acceptance Testing and Quality Control of Gamma Cameras, Including SPECT, *Journal of Nuclear Medecine*. **28(7)**, 1221-1227.

[17] Todd-Pokropek, A. (1983). Quality Control and Assurance of Single Photon Emission Computerized Tomographic Systems, *Annals of Radiology*. **26(1)**, 23-30.

[18] Hutton, B. F., Erlandsson, K., Thielemans, K. (2018). Advances in Clinical Molecular Imaging Instrumentation, *Clinical and Translational Imaging*. **6(1)**, 31-45.

[19] Lees, J. E., Bassford, D. J., Blackshaw, P. E., Perkins, A. C. (2010). Design and Use of Mini-Phantoms for high Resolution Planar Gamma Cameras, *Applied Radiation and Isotopes*. **68(12)**, 2448-2451.

[20] Saxena, S. K., Kumar, Y., Malpani, B., Rakshit, S., Dash, A. (2016). Development of a Phantom and Assessment of 141Ce as a Surrogate Radionuclide for Flood Field Uniformity Testing of Gamma Cameras, *Applied Radiation and Isotopes*, **(112)**. 115-121.

[21] Söderberg, M., Engeland, U., Mattsson, S., Ebel, G., Leide-Svegborn, S. (2011). Initial Tests of a New Phantom for Investigation of Spatial Resolution, Partial Volume Effect and Detectability in Nuclear Medicine Tomography. *Journal Of Physics: Conference Series*. (317, 1). 012017. IOP Publishing.

[22] Sokole, E. B., Płachcínska, A., Britten, A. (2010). Acceptance Testing for Nuclear Medicine Instrumentation. *European Journal of Nuclear Medicine and Molecular Imaging*. **37(3)**, 672-681.

[23] Groch, M. W., Erwin, W. D. (2001). Single-photon Emission Computed Tomography in the Year 2001: Instrumentation and Quality Control. *Journal of Nuclear Medicine Technology*. **29(1)**, 12-18.

[24] Alqahtani, M. S., Lees, J. E., Bugby, S. L., Samara-Ratna, P., Ng, A. H., Perkins, A. C. (2017). Design and Implementation of a Prototype Head and Neck Phantom for the Performance Evaluation of Gamma Imaging Systems. *European Journal of Nuclear Medicine and Molecular Imaging Physics*. **4(1)**, 1-17.

[25] NEMA. National Electrical Manufacturers Association. (2012). NEMA Standards Publication NU-1 2012 Performance Measurements of Gamma Cameras. *Rosslyn, VA*.

[26] Van Staden, J. A., Du Raan, H., Lötter, M. G., Van Aswegen, A., Herbst, C. P. (2007). Production of Radioactive Quality Assurance Phantoms Using a Standard Inkjet Printer, *Physics in Medicine & Biology*. **52(15)**, 329-337.

[27] Zeinali, H., Ghiassi-Nejad, M., Mirzaii, A. (2007). Design an Adaptive Quality Control Phantom to Optimize QC Test Methods. *The Open Medical Imaging Journal*. **1(1)**, 1-6.

[28] Gar-elnabi, M. E., Ali, W. M., Ali Omer, M. A., Edam, G. A. (2015). Assessment of Gamma Camera SPECT Resolution Using Developed Quality Control Phantom. *International Journal of Science and Research*. **4(2)**, 2117-2121.

[29] Ng, A. H., Ng, K. H., Dharmendra, H., Perkins, A. C. (2009). A Low-cost Phantom for Simple Routine Testing of Single Photon Emission Computed Tomography (SPECT) Cameras. *Applied Radiation and Isotopes*. **67(10)**, 1864-1868.

[30] Perkins, A. C., Clay, D., Lawes, S. C. (2007). A Simple Low cost Phantom for the Quality Control of SPECT Cameras. *World Journal of Nuclear Medicine*. **6(1)**, 35-39.

[31] Lewellen, T. K., Graham, M. M. (1981). A Low-contrast Phantom for Daily Quality Control. *Journal of Nuclear Medicine: Official Publication, Society of Nuclear Medicine*. **22(3)**, 279-282.

[32] Malayeri, A. A., El Khouli, R. H., Zaheer, A., Jacobs, M. A., Corona-Villalobos, C. P., Kamel, I. R., Macura, K. J. (2011). Principles and Applications of Diffusion-weighted Imaging in Cancer Detection, Staging, and Treatment Follow-up. *Radiographics*. **31(6)**, 1773-1791.

[33] Mitra, A. (2016). *Fundamentals of Quality Control and Improvement*. John Wiley & Sons.

[34] EANM. EANM. European Association of Nuclear Medicine. 2007. Best Practice in Nuclear Medicine Part 2. A Technologist's Guide. A Technologist's Guide - Part 2, 1–48. Retrieved from papers2://publication/uuid/2AFC29D5-9E29-4E7A-9AA1-1CD066831D28.

[35] Hunt, D. C., Easton, H., Caldwell, C. B. (2009). Design and Construction of a Quality Control Phantom for SPECT and PET Imaging. *Medical Physics*. **36(12)**, 5404-5411.

[36] Branham, T. (2007). WE-A-M100J-02: Phantom Testing. *Medical Physics*, **34(6Part19)**, 2578-2578.

[37] Frame, P. W. (2004). A History of Radiation Detection Instrumentation. *Health Physics*. **87(2)**. 111-135.

[38] Seidlin, S. M., Marinelli, L. D., Oshry, E. (1946). Radioactive Iodine Therapy: Effect on Functioning Metastases of Adenocarcinoma of the Thyroid. J*ournal of the American Medical Association*. **132(14)**. 838-847.

[39] Seidlin, S. M., Marinelli, L. D., Oshry, E. (1990). Radioactive Iodine Therapy: Effect on Functioning Metastases of Adenocarcinoma of the Thyroid. *CA: A cancer Journal for Clinicians*. **40(5)**. 299-317.

[40] Cassen, B., Curtis, L., Reed, C. W. (1949). *A Sensitive Directional Gamma Ray Detector* (49). Oak Ridge, Tennessee: United States Atomic Energy Commission, Technical Information Service.

[41] Jaszczak, R. J., Coleman, R. E., Lim, C. B. (1980). SPECT: Single Photon Emission Computed Tomography. *IEEE Transactions on Nuclear Science*. **27(3)**, 1137-1153.

[42] Kharfi, F. (2013). Principles and Applications of Nuclear Medical Imaging: A Survey on Recent Developments. *Imaging and Radio analytical Techniques in Interdisciplinary Research, Fundamentals and Cutting Edge Applications*.

[43] Sharp, P. F., P. F. Sharp, H. G. Gemmell, A. D. Murray (Eds.). (2005). *Practical Nuclear Medicine*. Springer: London.

[44] L'Annunziata, M. F. (Ed.). (2012). *Handbook of Radioactivity Analysis*. Academic press.

[45] Gamma decay - Energy Education. (2020). Retrieved 27 September 2020, from https://energyeducation.ca/encyclopedia/Gamma_decay.

[46] Yeong, C. H., Cheng, M. H., Ng, K. H. (2014). Therapeutic Radionuclides in Nuclear Medicine: Current and Future Prospects. *Journal of Zhejiang University SCIENCE B*. **15(10)**, 845-863.

[47] Buvat, I., Frey, E., Green, A., Ljungberg, M. (2014). Quantitative Nuclear Medicine Imaging: Concepts, Requirements and Methods. *Human Health Reports, 9*.

[48] Fernandes, A. R., Oliveira, A., Pereira, J., Coelho, P. S. (2017). Nuclear Medicine and Drug Delivery. *Advanced Technology for Delivering Therapeutics*. **1**, 159.

[49] Alsharef, S., Alanazi, M., Alharthi, F., Qandil, D., Qushawy, M. (2020). Review About Radiopharmaceuticals: Preparation, Radioactivity, and Applications. *International Journal of Applied Pharmaceutics*. **12(3)**, 8-15.

[50] Boschi, A., Uccelli, L., Martini, P. (2019). A Picture of Modern Tc-99m Radiopharmaceuticals: Production, Chemistry, and Applications in Molecular Imaging. *Applied Sciences*. **9(12)**, 2526.

[51] Podgoršak, E. B. (2014). Interaction of Photons with Matter. *In Compendium to Radiation Physics for Medical Physicists* (387-514). Springer: Berlin, Heidelberg.

[52] Bushberg, J. T., Boone, J. M. (2011). *The Essential Physics of Medical Imaging*. Lippincott Williams & Wilkins.

[53] Sorenson, J. A., Phelps, M. E. (1987). *Physics in Nuclear Medicine* (115-121). New York: Grune & Stratton.

[54] Dance, D. R., Christofides, S., Maidment, A. D. A., McLean, I. D., Ng, K. H. (2014). Diagnostic radiology physics: A handbook for teachers and students. Endorsed by: American Association of Physicists in Medicine, Asia-Oceania Federation of Organizations for Medical Physics, European Federation of Organisations for Medical Physics. *International Atomic Energy Agency (IAEA)*: *IAEA*.

[55] Cunningham, J. R., & Dance, D. R. (2013). Diagnostic Radiology Physics: A Handbook for Teachers and Students, chapter Interaction of radiation with matter. *International Atomic Energy Agency, Viena.*

[56] Peterson, T. E., Furenlid, L. R. (2011). SPECT Detectors: The Anger Camera and Beyond. *Physics in Medicine & Biology*. **56(17)**, 145-182.

[57] Gemmell, H. G., Murray, A. D., Sharp, P. F. (2006). *Practical Nuclear Medicine*. Springer.

[58] Madsen, M. T. (2006). Anger Camera. *Encyclopedia of Medical Devices and Instrumentation*.

[59] Percuoco, R. (2014). Plain Radiographic Imaging. *In Clinical Imaging* (1-43). Elsevier: Mosby.

[60] Mettler Jr, F. A., Guiberteau, M. J. (2012). *Essentials of Nuclear Medicine Imaging: Expert Consult-Online and Print*. Elsevier Health Sciences.

[61] Cherry, S. R., Sorenson, J. A., Phelps, M. E. (2012). *Physics in Nuclear Medicine e-Book.* Elsevier Health Sciences.

[62] Cherry, S. R., Sorenson, J. A., Phelps, M. E. (2012). The Gamma Camera: Basic Principles. *Physics in Nuclear Medicine, 3*.

[63] Bailey, D. L., Humm, J. L., Todd-Pokropek, A., Aswegen, A. V. (2014). Nuclear Medicine Physics: A Handbook for Teachers and Students. Endorsed by: American Association of Physicists in Medicine (AAPM), Asia–Oceania Federation of Organizations for Medical Physics (AFOMP), Australasian College of Physical Scientists and Engineers in Medicine (ACPSEM), European Federation of Organisations for Medical Physics (EFOMP), Federation of African Medical Physics Organisations (FAMPO), World Federation of Nuclear Medicine and Biology (WFNMB).

[64] The Gamma Camera: Performance Characteristics. (2020). Retrieved 27 September 2020, from https://radiologykey.com/the-gamma-camera-performance-characteristics.

[65] Zanzonico, P. (2012). Principles of Nuclear Medicine Imaging: Planar, SPECT, PET, Multi-modality, and Autoradiography Systems. *Radiation Research*. **177(4)**, 349-364.

[66] Eisaman, M. D., Fan, J., Migdall, A., Polyakov, S. V. (2011). Invited Review Article: Single-photon Sources and Detectors. *Review of Scientific Instruments*. **82(7)**, 071101.

[67] Diehl, R. (2001). Gamma-ray Production and Absorption Processes. *In The Universe in Gamma Rays* (9-25). Springer: Berlin, Heidelberg.

[68] Penelope, A. R., Williams, J. (2008). *Farr's Physics for Medical Imaging*. Saunders Elsevier.

[69] Saha, G. B. (2006). Radiation Biology. *In Physics and Radiobiology of Nuclear Medicine* (226-267). Springer: New York, NY.

[70] Hemmati, H., Kamali-Asl, A., Haghshenas, R. (2015). The Effects of Light Guide Thickness on the Accuracy of Position Estimation, Linearity, and Uniformity Responses of Anger Camera: a Monte Carlo Study. *Frontiers in Biomedical Technologies*. **2(3)**, 172-183.

[71] Chandra, R., Rahmim, A. (2017). *Nuclear Medicine Physics: The Basics*. Lippincott Williams, Wilkins.

[72] Saha, G. B. (2001). Imaging Devices. *In Physics and Radiobiology of Nuclear Medicine* (100-110). Springer: New York, NY.

[73] Wang, Y. (2014). Nuclide Imaging: Planar Scintigraphy, SPECT, PET. *Polytechnic University, Brooklyn. Disponível em:< http://eeweb. poly. edu/~ yao/EL5823/NuclearImaging_ch8_9. pdf>, Acesso em, 27*.

[74] Khalil, M. (Ed.). (2010). *Basic Sciences of Nuclear Medicine*. Springer Science, Business Media.

[75] Zaidi, H. (2006). Recent Developments and Future Trends in Nuclear Medicine Instrumentation. *Zeitschrift für Medizinische Physik*. **16(1)**, 5-17.

[76] Radiology Key. Fastest Radiology Insight Engine. Available at: https://radiologykey.com/the-gamma-camera-basic-principles. 26.2.2016.

[77] Ravi, M., Theja, K. H., Sivaramakrishnan, S., Sai, S. S. S., Sai, K. V. (2014). Fully Digital Gamma Camera for Small Organ Imaging. *Quantum*. **76(98)**, 128.

[78] Saha, G. B. (2006). Digital Computers in Nuclear Medicine. *In Physics and Radiobiology of Nuclear Medicine* (139-152). Springer: New York, NY.

[79] Parker, J. A., Daube-Witherspoon, M. E., Graham, L. S., Royal, H. D., Todd-Pokropek, A. E., Yester, M. V. (2004). *Society of Nuclear Medicine Procedure Guideline for General Imaging*.

[80] Rojas, G. M., Quintana, J. C., Jer, J., Astudillo, S., Arenas, L., Araya, H. (2004). Analog Gamma Camera Digitalization Computer System. *Revista Espanola de Medicina Nuclear*. **23(2)**, 106.

[81] Computer Interfacing and Image Processing. (2020). Retrieved 27 September 2020, from https://basicmedicalkey.com/computer-interfacing-and-image-processing.

[82] Kharfi, F. (2013). Principles and Applications of Nuclear Medical İmaging: A Survey on Recent Developments. *Imaging and Radioanalytical Techniques in Interdisciplinary Research—Fundamentals and Cutting Edge Application.*

[83] Knoll, P., Rahmim, A., Gültekin, S., Šámal, M., Ljungberg, M., Mirzaei, S., Szczupak, B. (2017). Improved Scatter Correction with Factor Analysis for Planar and SPECT Imaging. *Review of Scientific Instruments*. **88(9)**, 094303.

[84] Asgari, A., Ashoor, M., Sarkhosh, L., Khorshidi, A., Shokrani, P. (2019). Determination of Gamma Camera's Calibration Factors for Quantitation of Diagnostic Radionuclides in Simultaneous Scattering and Attenuation Correction. *Current Radiopharmaceuticals*. **12(1)**, 29-39.

[85] IAEA. International Atomic Energy Agency. (2009). *Quality Assurance for SPECT Systems, Human Health Series No. 6, IAEA*, Vienna.

[86] Soni, P. S. (1992). *Quality Control of Imaging Devices* (No. NMS--1). International Atomic Energy Agency (IAEA).

[87] Moreno, A. M., Laguna, A. R., Zamudio, F. E. T. (2012). Implementation of Test for Quality Assurance in Nuclear Medicine Gamma Camera. *In AIP Conference Proceedings.* **1494(1)**, 88-90. American Institute of Physics.

[88] Erwin, W. D. (2004). IAEA Quality Control Atlas for Scintillation Camera Systems. *Journal of Nuclear Medicine*. **45(10)**, 1792-1792.

[89] IAEA. International Atomic Energy Agency. (1991). *Quality Control of Nuclear Medicine Instruments 1991, IAEA-TECDOC-602*, IAEA. Vienna.

[90] Dondi, M., Paez, D., Torres, L., Marengo, M., Delaloye, A. B., Solanki, K., Pascual, T. (2018). Implementation of Quality Systems in Nuclear Medicine: Why it matters. An Outcome Analysis (Quality Management Audits in Nuclear Medicine Part III). *In Seminars in nuclear medicine,* **48(3)**, 299-306. WB Saunders.

[91] Meghzifene, A., Sgouros, G. (2013). IAEA Support to Medical Physics in Nuclear Medicine. *In Seminars in Nuclear Medicine*, **43(3)**, 181-187.

[92] Raff, U., Spitzer, V. M., Hendee, W. R. (1984). Practicality of NEMA Performance Specification Measurements for User-based Acceptance Testing and Routine Quality Assurance. *Journal of Nuclear Medicine*. **25(6)**, 679-687.

[93] Saha, G. B. (2013). Performance Parameters of Gamma Cameras. *In Physics and Radiobiology of Nuclear Medicine.* (127-151). Springer: New York, NY.

[94] NEMA. National Electrical Manufacturers Association. (2001). NEMA Standards Publication NU 1-2001, *Performance Measurements of Scintillation Cameras*. Available at: https://standards.globalspec.com/std/1628229/nema-nu-1.

[95] Anizan, N., Wang, H., Zhou, X. C., Hobbs, R. F., Wahl, R. L., Frey, E. C. (2014). Factors Affecting the Stability and Repeatability of Gamma Camera Calibration for Quantitative Imaging Applications Based on a Retrospective Review of Clinical Data. *European Journal of Nuclear Medicine and Molecular Imaging Research*. **4(1)**, 67.

[96] AAPM. American Association of Physicists in Medicine. (2017). THE REPORT OF AAPM TASK GROUP 177: *Acceptance Testing and Annual Physics Survey Recommendations for Gamma Camera*, SPECT, and SPECT/CT Systems. Avalaible at: https://aapm.org/pubs/reports/detail.asp?docid=184.

[97] AAPM. American Association of Physicists in Medicine. (1987). Rotating Scintillation Camera SPECT Acceptance Testing and Quality Control, AAPM report No:22, College Park, MD. Available at: https://aapm.org/pubs/reports/RPT_22.pdf.

[98] Siegel, J. A., Benedetto, A. R., Jaszczak, R. J., Lancaster, J. L., Madsen, M. T., Woodsen, W. W., Zimmerman, R. E. (1987). Rotating Scintillation Camera SPECT Acceptance Testing and Quality Control. *American Association of Physicists in Medicine. New York, NY.*

[99] Simeonov, G. (2013). Criteria for Acceptability of Medical Radiological Equipment in Euratom Legislation. *Radiation Protection Dosimetry*. **153(2)**, 147-149.

[100] Bergmann, H. (1993). Test Phantoms in Nuclear Medicine: Planar Gamma Camera. *Radiation Protection Dosimetry*. **49(1-3)**, 285-293.

[101] A. K. (2017). Quality Control of Gamma Camera with SPECT Systems. *International Journal of Medical Physics, Clinical Engineering and Radiation Oncology*. **6(03)**, 225.

[102] IEC. International Electrotechnical Commission. (1998). Radionuclide Imaging Devices-Characteristics and Test Conditions. Part 1. Positron Emission Tomographs. *EC Standard 61675-1*.

[103] Plastic, acrylic and plexiglass - we explain the difference - Akriform. (2020). Retrieved 28 September 2020, from https://akriform.com/news/plastic-acrylic-and-plexiglass-we-explain-the-difference.

[104] Plexiglas. (2020). Retrieved 28 September 2020, from https://b2b.partcommunity.com/community/knowledge/en/detail/1763/Plexiglas#knowledge_article.

[105] Chung, J. P., Seong, Y. M., Kim, T. Y., Choi, Y., Kim, T. H., Choi, H. J., Chung, H. T. (2018). Development of a PMMA Phantom as a Practical Alternative for Quality Control of Gamma knife® Dosimetry. *Radiation Oncology*. **13(1)**, 176.

[106] Sandborg, M. (1990). Comparison Between Lucite and Water as a Phantom Material in Medical Radiology. *Progress in Nuclear Energy*. **24(1-3)**, 355-364.

[107] Oumar, A. A., Erçelebi, E. (2020). Assessment of an In-house Phantom for the Quality Control of a Clinical Gamma Camera. *Journal of X-Ray Science and Technology*. **28(3)**, 461-470.

[108] Philips. 2020. Philips Healthcare | DICOM - Nuclear Medicine. Available at: <https://www.philips.com.tr/healthcare/resources/support-documentation/dicom-nuclear-medicine.>. Accessed 20.09.2020.

[109] Location selector | Philips. (2020). Retrieved 28 September 2020, from https://www.usa.philips.com/healthcare/country-selector.

[110] Hotel, D. R. (1980). American Association of Physicists in Medicine. *Medical Physics*, 7(4).

[111] AAPM Reports - Scintillation Camera Acceptance Testing & Performance Evaluation. (2020). Available at: https://www.aapm.org/pubs/reports/detail.asp?docid=5.

[112] Madsen, M. T. (2007). Recent Advances in SPECT Imaging. *Journal of Nuclear Medicine*. **48(4)**, 661-673.

CURRICULUM VITAE

PERSONAL INFORMATION

Family name:	Ahmat Oumar
First name:	Alio
Date and Place of Birth:	10 December 1988, Chad
Nationality:	Chad
Phone:	+905373523918
Email:	Aliofils10@yahoo.fr
Languages	Arabic, English, French, Turkish

EDUCATION

Degree	University	Year of graduation
Ph. D.	Gaziantep University Gaziante, TURKEY	2020
MS	Constantine University Constantine, ALGERIA	2013
BS	Constantine University Constantine, ALGERIA	2011

PUBLICATIONS

- Oumar, A. A., Erçelebi, E. (2020). Assessment of an In-house Phantom for the Quality Control of a Clinical Gamma Camera, Journal of X-Ray Science and Technology, 1(10), 461 – 470.